EXCITED STATES OF INDOLE AND AZAINDOLES

Thesis for the Degree of M. S.

MICHIGAN STATE UNIVERSITY
LI LILLIAN YANG

1974

ABSTRACT

EXCITED STATES OF INDOLE AND AZAINDOLES

By

Li Lillian Yang

Excited state characteristics of indole and various aza-substituted indoles, 2-, 3-, 4-, 5-, and 7-azaindoles, are studied. A comparative study of the absorption spectra in the gas phase and in solution as well as emission spectra at room and cryogenic temperatures has been performed. Both fluorescence and phosphorescence spectra and triplet state lifetimes are investigated. Various environments (solvents) are used and spectral shifts are interpreted in terms of various interactions, i.e., dispersion, dipole-induced dipole, dipole-dipole interactions and hydrogen bonding. These shifts are correlated with charge density changes at the aza and pyrrolic nitrogens. These charge densities are calculated using Pariser-Parr-Pople method. From the absorption and emission studies, excited state dipole moments and pK's are obtained.

The knowledge of the absorption and dissipation of excitation energy by these molecules is important in radiation biophysics and photobiology, and in using these molecules as fluorescent probes to probe changes in their natural environment. Information gained regarding the chemistry of the excited states of these molecules is valuable in further understanding of photoinduced proton transfer phenomenon.

EXCITED STATES OF INDOLE AND AZAINDOLES

By

Li Lillian Yang

A THESIS

Submitted to

Michigan State University

in partial fulfillment of the requirements

for the degree of

MASTER OF SCIENCE

Department of Biophysics

1974

To my parents

ACKNOWLEDGEMENTS

I would like to express my thanks to my research adviser, Prof. M. Ashraf El-Bayoumi, for his assistance with the work herein reported. Dr. El-Bayoumi has contributed greatly to the development of my scientific understanding. The constructive criticism and advice of the thesis committee members, Dr. E. McGroarty, Dr. A. Haug, and Dr. C. H. Suelter are also greatly appreciated. Special thanks go to my colleague and best friend, Dr. Ph. Avouris, for numerous discussions and encouragement.

This research was supported by the College of Osteopathic Medicine, with the cooperation of the Biophysics Department, Michigan State University, East Lansing, Michigan.

TABLE OF CONTENTS

LIST OF TABLES

LIST OF FIGURES

CHAPTER 1

GENERAL INTRODUCTION

Indole is a unique and important molecule to both biochemists and biophysicists. It is the chromophore of tryptophan, an amino acid found in most proteins. Among the three amino acids that absorb light in the ultraviolet region, tryptophan has a maximum extinction coefficient of 700 (at 280 nm) which is five times that of tyrosine (at 278 nm) and fifteen times that of phenylalanine (at 260 nm). Thus, tryptophan accounts for most of the direct energy deposition from UV irradiation in protein. Indole is also the chromophore of many other important biological substances like: serotonin (a transmitter substance found at chemical synapses between neurons), indole acetic acid (a plant growth hormone), and lysergic acid (LSD), bufotenin and psilocybin (hallucinogenic drugs).

Purine an important biological molecule is an aza-substituted indole (3,5,7-triazaindole). Purine is the chromophore for adenine and guanine, two of the bases found in DNA and RNA. Purine is also the chromophore of ATP and NAD coenzymes.

Azaindoles are of interest as possible metabolite antagonists of purine and of physiologically active indoles such as serotonin, tryptophan, and NN-diehyl-lysergamide. Competition has been demonstrated between 7-azaindole and indoles in bacteria, viruses, fungi, and protozoa. 7-Azatryptophan has been incorporated into bacterial protein in the place of tryptophan by a tryptophan-requiring mutant of *E. coli*, but growth soon ceased[1].

T2 bacteriophages behave somewhat similarly[1], 7-azaindole inhibits the conversion of indole into tryptophan in the mould Neurospora crassa[2], and 7-azatryptophan prevents the uptake of tryptophan by the protozoon Tetrahymena pyriformis.[3] These compounds should be of considerable interest in other systems, particularly those in which tryptophan synthesis is carried out, for it should be possible there to determine more exactly the point of interference.

In view of their importance, it is not surprising to see that the spectroscopy of indole has attracted great attention. Our spectral study of indole and various aza-substituted indoles, 2-, 3-, 4-, 5-, and 7-azaindole, include detailed studies of the solution absorption and emission spectra of these molecules at room and cryogenic temperatures. Both fluorescence spectra and phosphorescence spectra and lifetimes are studied. Various environment (solvents) are used and spectral shifts are interpreted in terms of various interactions, i.e., dispersion, dipole-induced dipole interaction, dipole-dipole interaction and hydrogen bonding interaction. These shifts are correlated with charge density changes at the aza and pyrrolic nitrogens. These charge densities are calculated by using Pariser-Parr-Pople method. The results of this investigation should be helpful in the area of radiation biophysics because of the knowledge we gained on the way these molecules dissipate the light energy they absorb and the effect of the environment on these processes. An understanding of the spectroscopy and the effect of the environment on the emissive properties of molecules like indole (tryptophan) will improve their use as intrinsic fluorescent probes in proteins for the study of processes like denaturation, dimerization, etc. Gas phase absorption spectra of these molecules have also been studied. The analysis of these

spectra is helpful in identifying electronic transitions and in studying the effect of aza-nitrogen substitution on the spectra.

CHAPTER 2

EXPERIMENTAL

(A) Compounds Studied

Molecules studied here are: indole, 2-, 3-, 4-, 5-, and 7-azaindoles (Figure 1). The means of purification are described below for each molecule.

(1) Indole: purchased from Calbiochem was recrystallized once from an alcohol-water mixture then vacuum sublimed slowly (one day).

(2) 2-Azaindole (Benzpyrazole): purchased from Aldrich was recrystallized two times from water.

(3) 3-Azaindole (Benzimidazole): purchased from Aldrich was recrystallized in water then vacuum sublimed slowly.

(4) 4-Azaindole: 4-azaindole oxalate salt was kindly supplied by Dr. Nachod of Sterling-Winthrop Research Institute. The salt was liberated by Na_2CO_3, then the free 4-azaindole was extracted by ether, and was further purified by sublimation and recrystallization.

(5) 5-Azaindole: kindly supplied by Dr. Nachod of Sterling-Winthrop Research Institute, was vacuum sublimed slowly.

(6) 7-Azaindole: purchased from Aldrich was recrystallized from cyclohexane three times.

(B) Purification of Solvents

(1) Water: double distilled water was used.

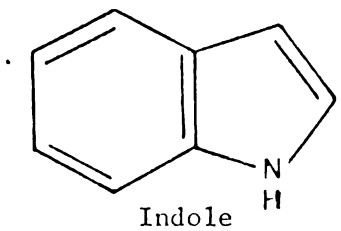

Indole

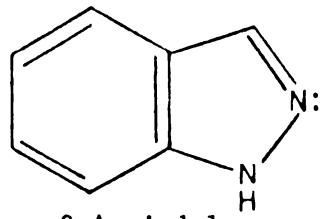

2-Azaindole

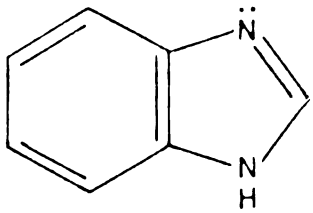

3-Azaindole

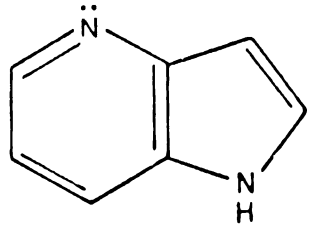

4-Azaindole

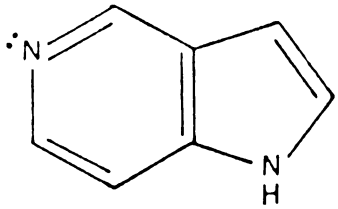

5-Azaindole

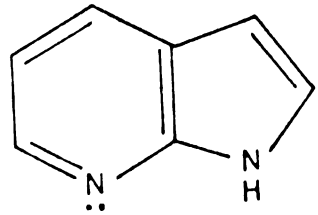

7-Azaindole

Figure 1. Experimentally Studied Compounds

(2) Ethanol: 200 proof ethanol was fractionally distilled. When the UV absorption spectrum in 10 cm cell did not show any benzene absorption, the ethanol was considered pure. Ethanol was kept refluxing and freshly distilled when needed.

(3) Diethyl Ether: Anhydrous ether was refluxed over Na ribbons, then distilled in a 1 meter column.

(4) 3-Methylpentane (3MP): A modified method of Pott[4] was used. Phillips Pure Grade 3MP was mixed with 50:50 sulfuric acid and nitric acid, stir overnight. Repeat by only using concentrated sulfuric acid until reddish color is gone. Neutralization by stirring with diluted Na_2CO_3 for one hour was followed by stirring with distilled water and stored over $CaCl_2$. The solvent was then refluxed over Na ribbon and distilled through 1 meter column.

(C) Spectral Measurements

(1) Absorption Spectra: all UV absorption spectra were taken on a Cary 15 spectrophotometer with a resolution of about 1 Å. A 10 cm absorption cell with quartz window was used for vapor spectra. This modified cell was wrapped with nichrome wire which was secured with silicone cement. Vacuum stopcock was attached to the only opening of the absorption cell to provide a 10^{-6} Torr when connected to the vacuum line. For solution absorption spectra, 1 cm path length cells were used in all cases. A matched cell

were used as reference.

(2) Emission Spectra: emission spectra were determined using an Aminco-Keirs spectrophotophosphorimeter equipped with a high pressure xenon arc lamp and IP21 phototube. Some of the samples were degassed prior to their use in luminescence studies. This was done by freezing the sample with liquid nitrogen, evacuation above the sample to a pressure of about 10^{-6} Torr, allowing the sample to thaw, then refreezing and continuing this freeze-thaw cycle until the vacuum line ionization gauge did not quiver when the stop-cock was opened after a freeze.

CHAPTER 3

VAPOR SPECTRA OF INDOLE AND AZAINDOLES

Vapor spectra of indole, 2-, 3-, 4-, 5-, and 7-azaindoles were measured. Our purpose is to study the effect of aza-substitution at different positions on the energy and intensities of the low energy absorption bands. These energy changes will be correlated with charge densities changes as a result of excitation, the latter are calculated using Pariser-Parr-Pople method. Moreover this correlation study is helpful in identifying electronic transitions, particularly in cases where absorption bands greatly overlap.

Introduction

Describing the molecule, with N atomic nuclei, in terms of a Born-Oppenheimer state function which separates the electronic and nuclear motion, one writes:

$$\Psi(q,Q) = \psi_e(q,Q)\psi_v(Q) \tag{1}$$

with the vibrational state function Ψ_v, depending only on the nuclear corrdinates, Q, whereas the electronic state function Ψ_e, depends on electronic coordinate, q, and the nuclear coordinates, Q, the independence of the electronic and nuclear motions implies that the electronic energy E_e and vibrational energy E_v will simply add to give the total energy of a vibronic state:

$$E = E_e + E_v \tag{2}$$

Each of the 3N-6 vibrations in a polyatomic molecule may be described in

terms of displacements along normal coordinates of the molecule. The vibrational energy states can be described approximately by a simple one-dimensional harmonic oscillator expression that is used for diatomic molecules, so the nth vibrational mode

$$E_{v_n} = (v + \tfrac{1}{2})h\nu_n \qquad v_n = 0,1,2,\ldots\ldots \quad (3)$$

v_n is the vibration quantum number for n^{th} vibrational mode, ν_n is its fundamental frequency. If the vibrational modes are independent of each others, the total energy of the molecule can be expressed as

$$E = E_e + \sum_{n=1}^{3N-6} (v_n + \tfrac{1}{2})h\nu_n \quad (4)$$

When a transition occurs between two vibronic levels, the change in energy

$$\Delta E = E_e + \sum_{m=1}^{3N-6} (v_m' + \tfrac{1}{2})h\nu_m' - \sum_{n=1}^{3N-6} (v_n'' + \tfrac{1}{2})h\nu_n'' \quad (5)$$

and in terms of wave numbers

$$\Delta E = \bar{\nu}_{oo} + \sum_{m=1}^{3N-6} \sum_{n=1}^{3N-6} (v_m'\bar{\nu}_m' - v_n''\bar{\nu}_n'') \quad (6)$$

with vibrational frequencies in the ground ($\bar{\nu}''$) and excited ($\bar{\nu}'$) electronic states, and the symbol $\bar{\nu}_{oo}$ being used to denote the transition between the zero vibrational level of one electronic state and the zero level of the other, i.e., when all the vibrational quantum numbers are zero.

The population distribution of each of the vibrational level is characterized by Boltzmann factor $e^{-E/kT}$. At room temperature $kT \simeq 210\ cm^{-1}$ and since the energy differences between vibrational states in organic molecules vary from two to twenty times this energy, the majority of molecules will be those for which $v_n'' = 0$. Therefore most of the absorption intensity will result from $v_n'' = 0$ molecules undergoing to the various excited vibronic states characterized by v_m' (Figure 2 and 3).

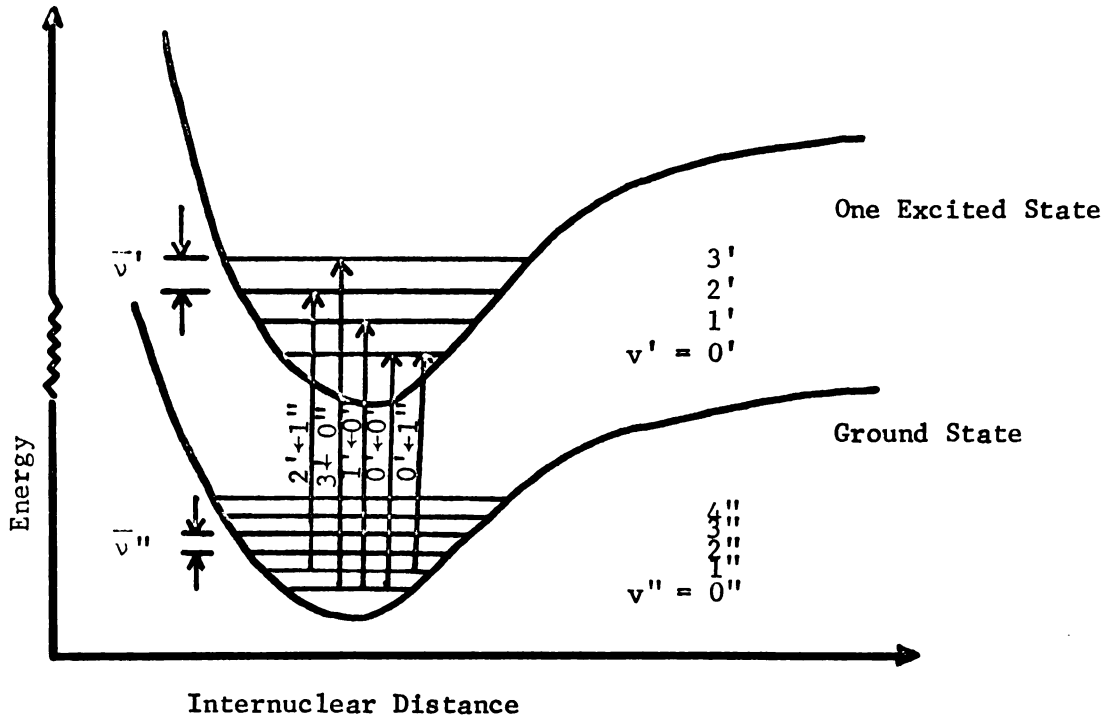

Figure 2. Ground and Excited State Potential Energy Curves and Vibronic Transitions.

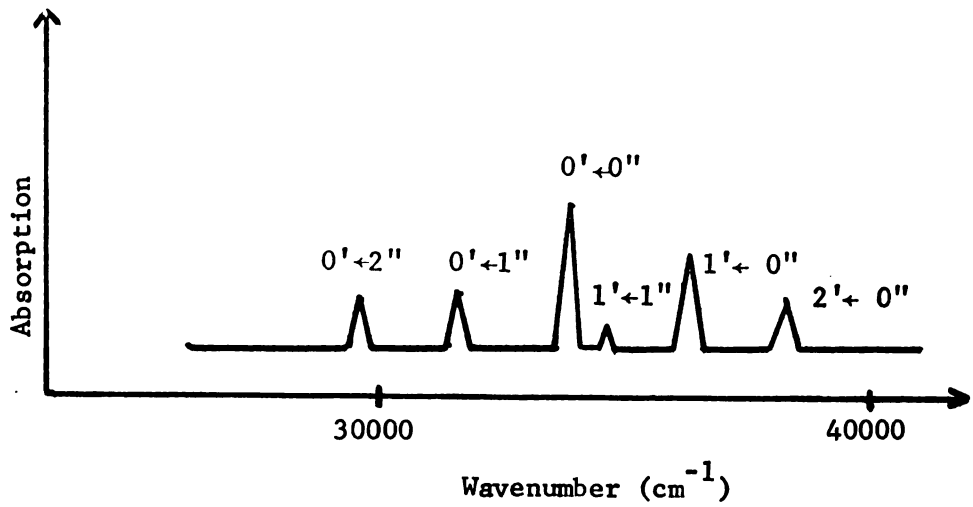

Figure 3. Schematic Absorption Band in a Vibronic Spectrum.

There is a fairly strong absorption progression approximately equally spaced, beginning with $0_m' \leftarrow 0''$ and continue to higher energies $v_m' \leftarrow 0''$ which are separated by the energy of excited state fundamental $\bar{\nu}_m'$. The concentration of other vibration level ($v'' > 0$) increases exponentially with temperature, the intensity of absorption bands resulting from molecules intially in other vibrational levels will also increase, these are called "hot bands". These bands characterized as $v_m' \leftarrow v_n''$ can be easily identified by their temperature dependence. For indole and aza-indoles with 3N-6 equals 42 and 39 respectively, therefore, one expects to see 42 or 39 progressions of excited state frequencies. It is also possible for combination frequencies to appear in which two vibrations are simultaneously excited during the transition. Considering the fine structure of each member in a progression, for instance the first member, if having only one quantum of vibrational energy ($v_n'' = 1$, all others $v_n'' = 0$) undergoes a transition to the excited electronic state with no vibrations excited (all $v_m' = 0$), this first member will be constructed with 42 or 39 fine structures. But from the transition probability:

$$P \propto \{\int_{-\infty}^{\infty} \Psi_e'(q,\bar{Q})\hat{M}(Q)\Psi_e''(q,\bar{Q})d\tau_q \int_{-\infty}^{\infty} \Psi_{v_m'}'(Q)\Psi_{v_n''}''(Q)\, d\tau_Q\}^2 \qquad (7)$$

with $\hat{M}(Q)$ as transition moment operator, and Born-Oppenheimer wave function for ground (Ψ'') and excited (Ψ') states. The first integral, electronic transition moment integral, determines the transition probability between electronic states Ψ_e' and Ψ_e''. The second integral is called the Franck-Condon overlap integral which determined the probability of the transition occured between particular vibrations characterized by v_m' and v_n''. It is found that the Franck-Condon factors for may of these transitions vanish identically or are very small, so that not all possible transitions between vibronic states will be observed. But for the

non-vanishing Franck-Condon integrals the magnitude determines the relative intensities of the vibronic bands which do appear. The assignment of transitions in the absorption spectra of nitrogen heterocyclic molecules is usually accomplished by comparing to spectra to those corresponding aromatic hydrocarbons. The perturbation on the energy level of an aromatic hydrocarbon caused by the substitution of a nitrogen atom into the ring is usually very small. Spectra of various polyacenes are similar and have been classified by Platt[5,6], they contain a symmetry-forbidden transition with long wavelength, low intensity, and allowed transition bands, with higher energy. The long-wavelength band is a long-axis polarized ^1L_b transition in the Platt[5] notation; slightly higher in energy is a short-axis polarized ^1L_a transition. There are situations where the ^1L_b and ^1L_a levels cross, e.g., naphthacene.

Substituting of an azanitrogen into the ring of an aromatic hydrocarbon causes small shifts in the energy levels. These shifts may be to longer or shorter wavelengths depending on the molecules, usually the shifts are small enough that the order of the energy level remains unchanged. This substitution destroys the symmetry property of the ^1L_b band, causes the transition to be less forbidden, in other words, substitution of nitrogen, intensifies the ^1L_b bands. Also $\pi^* \leftarrow n$ transition[7] is introduced as a result of aza-substitution. An $\pi^* \leftarrow n$ transition arises from a non-bonding σ- hybridized orbital to an anti-bonding π^* orbital. An $\pi^* \leftarrow n$ transition is generally lower in intensity than $\pi^* \leftarrow \pi$ transitions, and usually appears at longer wavelength than the lowest $\pi^* \leftarrow \pi$ transition. But when the molecule size increase the $\pi^* \leftarrow \pi$ band of aza-aromatic molecule shift to the red faster than $\pi^* \leftarrow n$, in this case the $\pi^* \leftarrow n$ transition is hidden under $\pi^* \leftarrow \pi$

bands. The magnitude of the shifts also depends on the direction of polarization of a given transition and the position of the substitution. The energy of an electronic transition is more greatly affected by substitution along the axis of polarization, thus the ^1L_b is more greatly affected by substitution in the β-positions, and ^1L_a by substitution in the α-positions.

Results and Discussions

Vapor spectrum of indole has been published by Hollas[8]. He assigned the ^1L_b 0-0 transition at 35233.2 cm^{-1}. The ^1L_b region of the 3-azaindole (benzimidazole) vapor spectrum has been published by Gordon and Yang[9]. Indole, 2-, 3-, and 7-azaindole vapor spectra have been taken earlier in our lab by Richard Wagner[10]. These spectra were repeated in addition the vapor spectra of 4-, and 5-azaindoles have been measured for the first time. Our purpose here is to compare these spectra and to investigate the effect of aza-substitution on energies and intensities of transitions. These energy changes will be correlated with charge densities calculated by using Pariser-Parr-Pople method.

Indole

Observation of the vapor spectrum (Figure 4) of indole indicates one region by sharp vibrational structure centered at 284 nm, and the other with diffuse vibrational structure centered at 260 nm. Using Platt notation[5], they correspond to $^1L_b \leftarrow {}^1A$ and $^1L_a \leftarrow {}^1A$ transition bands respectively. Hollas did not study the $^1L_a \leftarrow {}^1A$ transition. Our observation shows the ^1L_b 0-0 at 283.85 nm or 35229.8 cm^{-1} as the beginning of a sequence, another sequence starts at 278.2 nm or 720 cm^{-1} above the first sequence. Using this 720 cm^{-1} as a fundamental and goes to the blue, one can observe further sequences beginning at 272.2 nm and 267.3 nm. In addition one

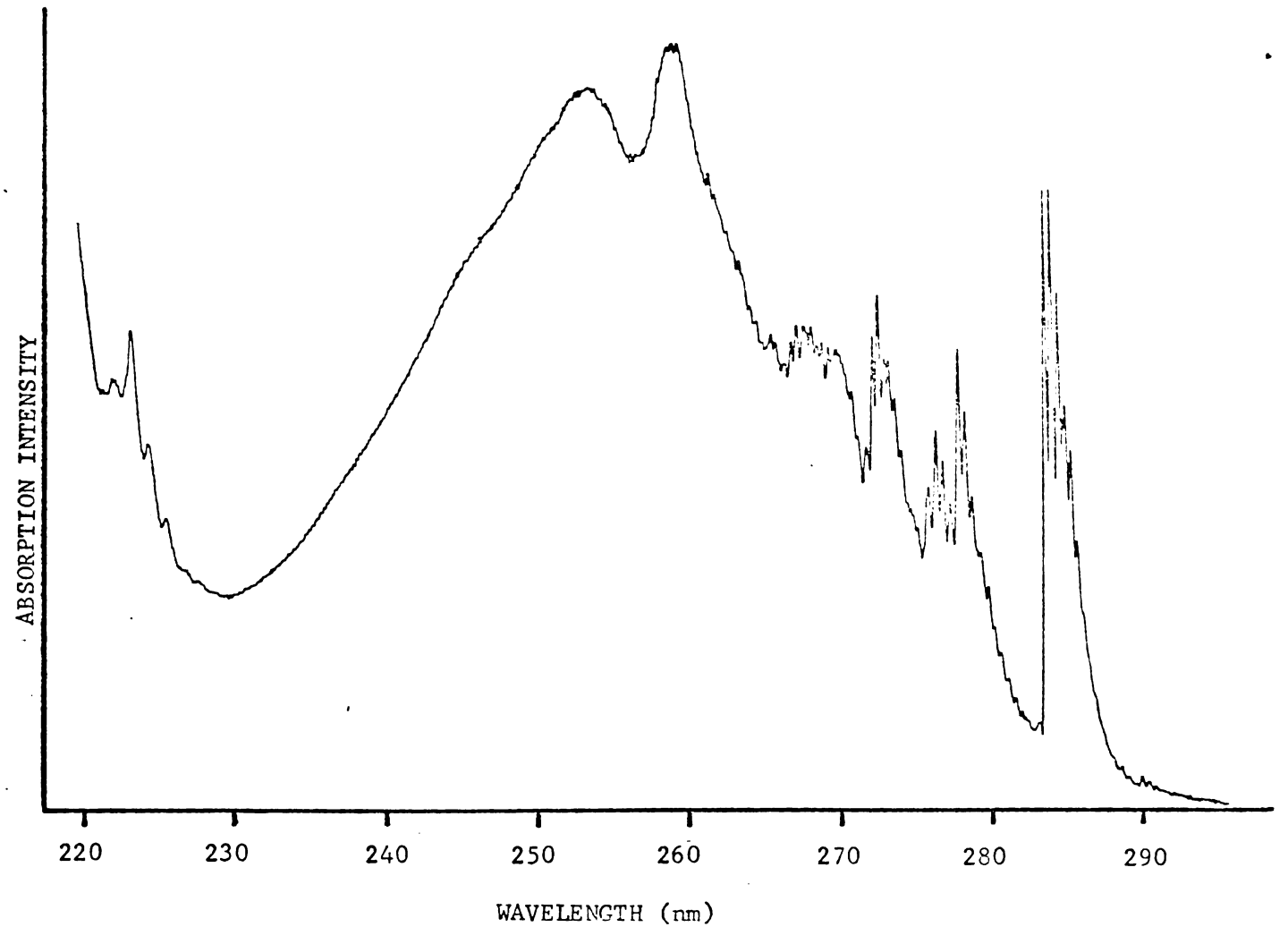

Figure 4. Indole Vapor Absorption Spectrum.

can observe two diffuse peaks at 253.8 nm and 259.8 nm with an energy separation of about 900 cm^{-1} which presumablly belong to the ^1L_a transition.

Azaindoles

Vapor spectrum of 2-azaindole shown in Figure 5 exhibits two electronic transition bands: one is characterized by sharp vibrational features centered at 285 nm, the other with diffuse vibrational structure centered at 245 nm. These two bands are quite well separated. The ^1L_b 0-0 transition is assigned at 290.3 nm or 34447.1 cm^{-1}. Other vibrational sequences start at 284.2 nm (35186.4 cm^{-1}), 279.2 nm (35816 cm^{-1}) and 273.7 nm (36536.3 cm^{-1}) with an average separation of 700 cm^{-1}. The diffuse band shows two peaks at 252.2 nm (39651 cm^{-1}) and 245.2 nm (40783 cm^{-1}) with 1100 cm^{-1} separation.

All other azaindoles, 3-, 4-, 5-, and 7-, are analysed in the same way, and both their vapor absorption spectra (Figure 5-9) and the corresponding peaks (Table 1) from experimental data as well as Pariser-Parr-Pople calculations[10] are shown in Table 2. From Wagner's[10] calculation, charge density in the ^1L_a and ^1L_b states are significantly different in indole (Figure 10). Considering the electronegativity, nitrogen is higher than carbon. Aza-substitutions of those places whose charge density increase show red shifts in the transition band. The charge density for the 2-, 4-, 5-, and 7-azaindoles increased in the ^1L_b state, the corresponding transitions are red shifted. This is also true for the ^1L_a state for 4-, and 7-azaindoles. Also there is a charge density decrease at both ^1L_a and ^1L_b state of 3 position of indole, the vapor spectrum shows blue shifted ^1L_a and ^1L_b bands. The charge density interpretation of vapor spectra agree qualitatively with the data. For further quantitative analysis, charge density becomes an unsatisfactory approximation.

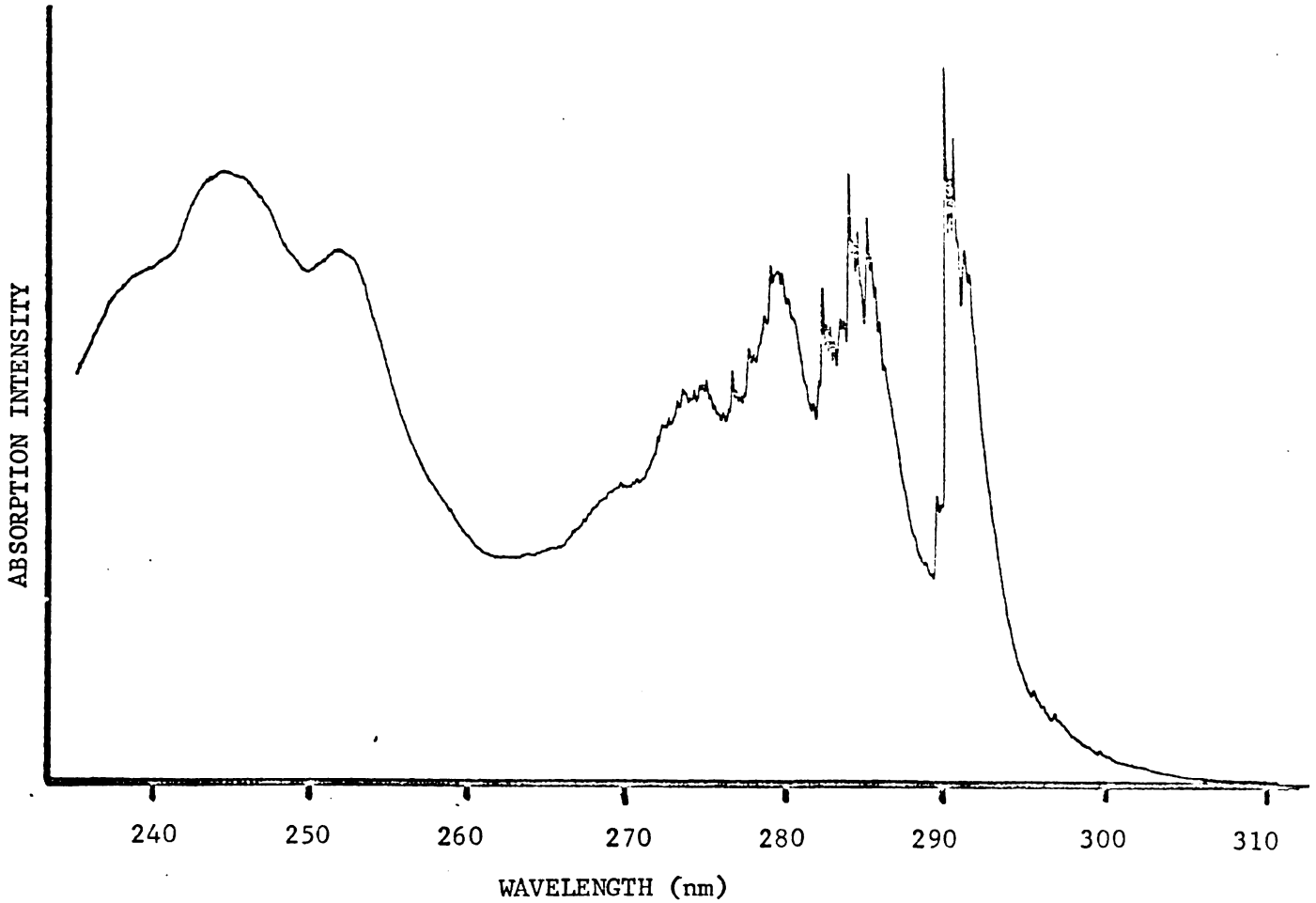

Figure 5. 2-Azaindole Vapor Absorption Spectrum.

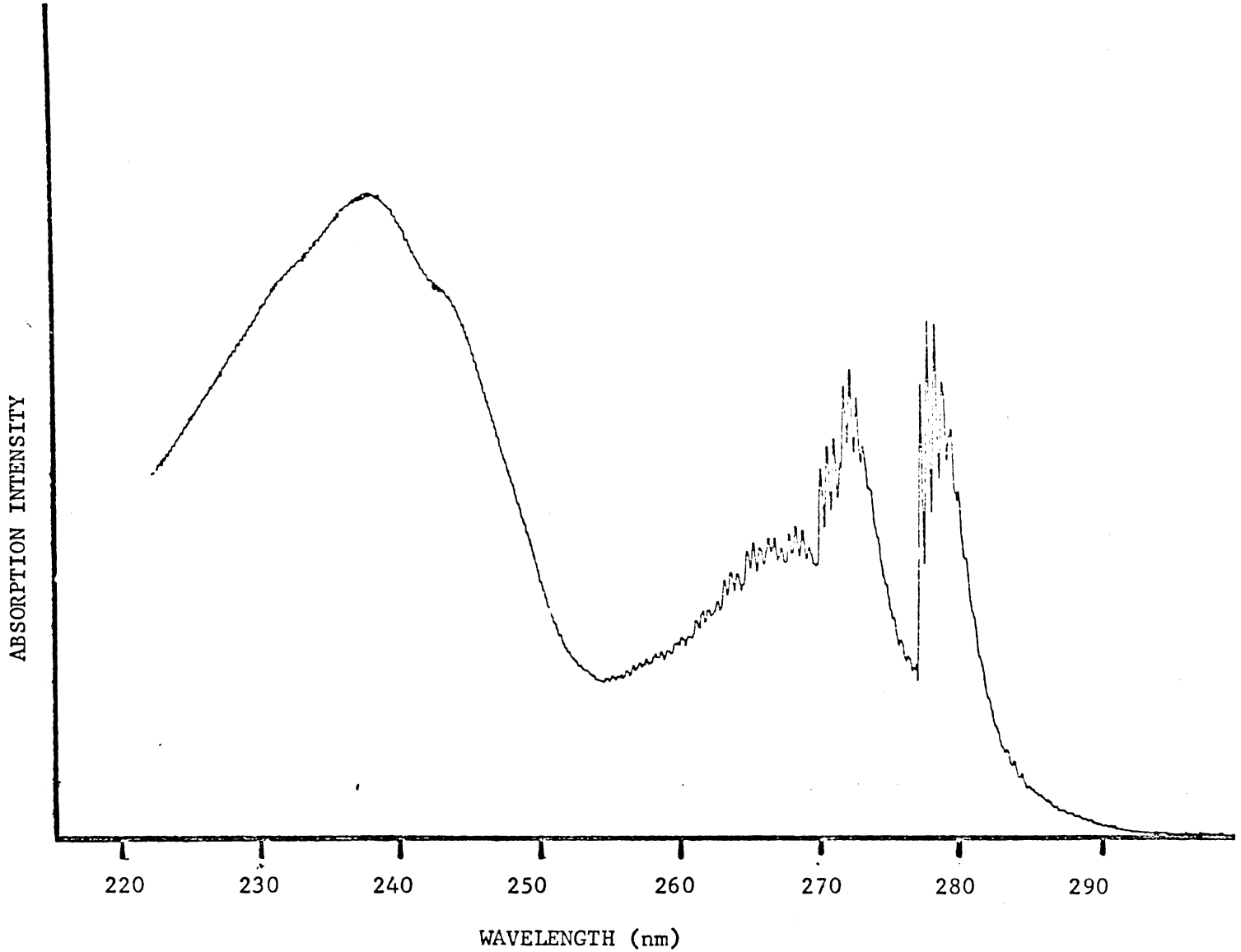

Figure 6. 3-Azaindole Vapor Absorption Spectrum.

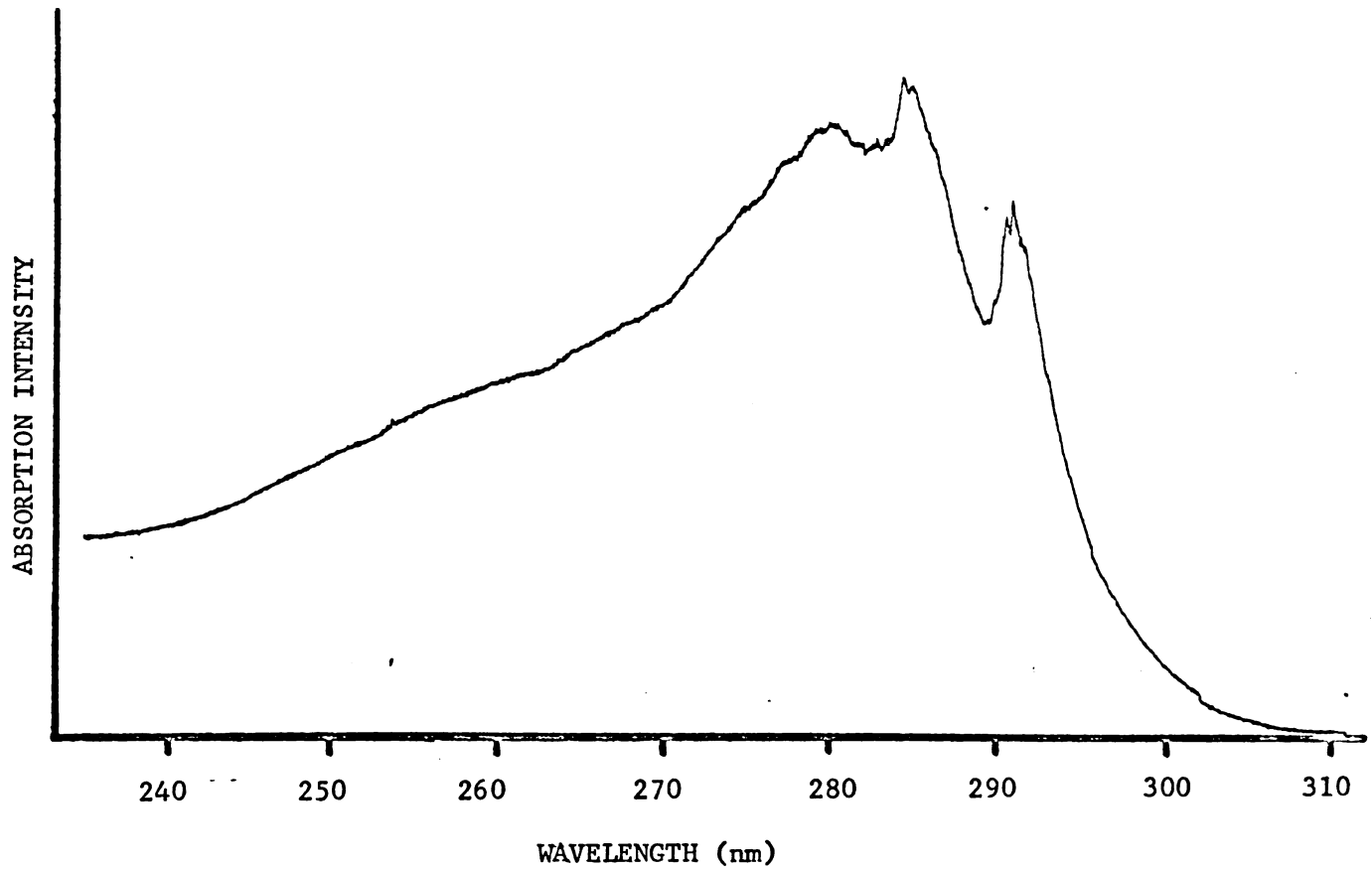

Figure 7. 4-Azaindole Vapor Absorption Spectrum.

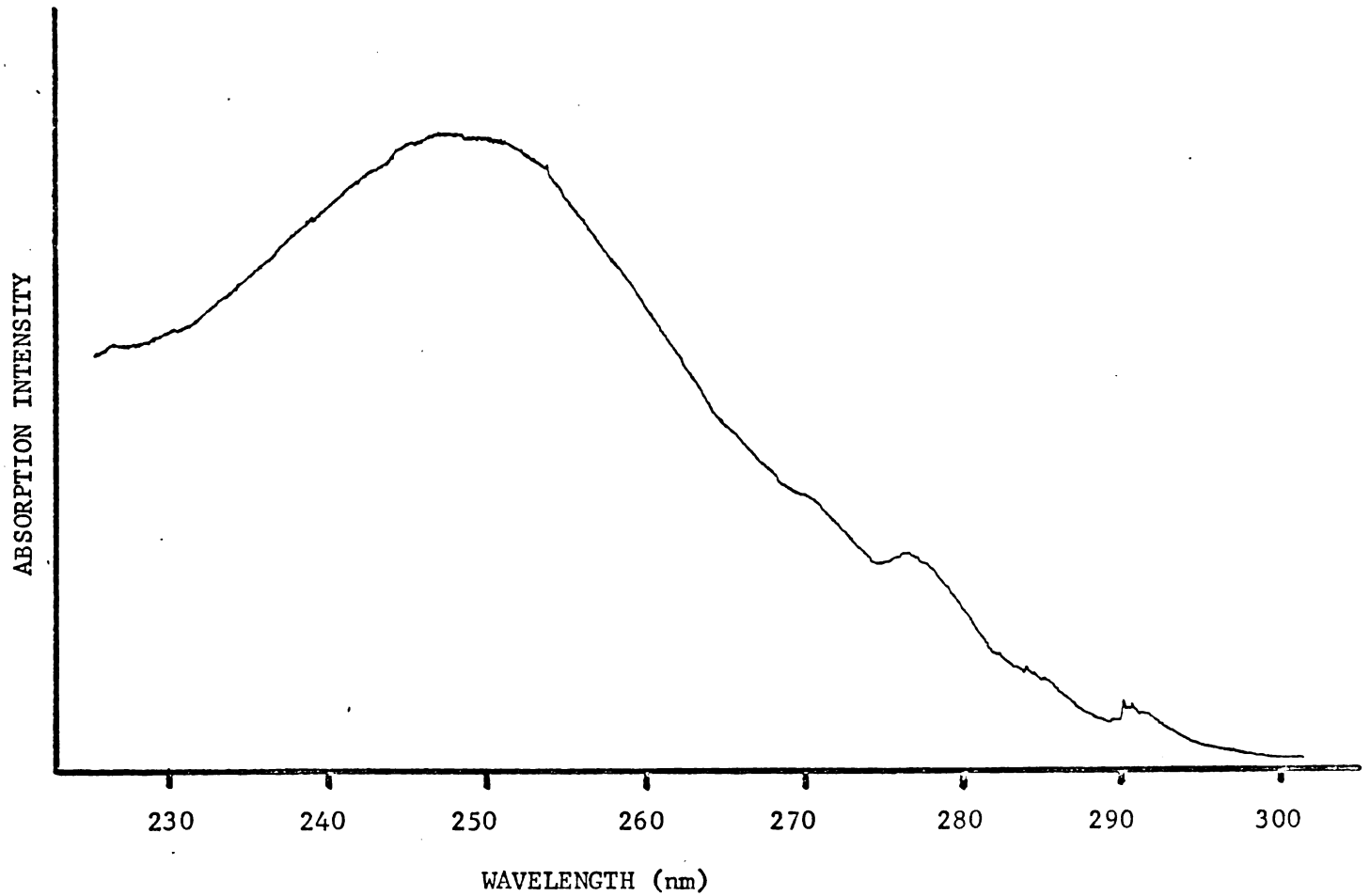

Figure 8. 5-Azaindole Vapor Absorption Spectrum.

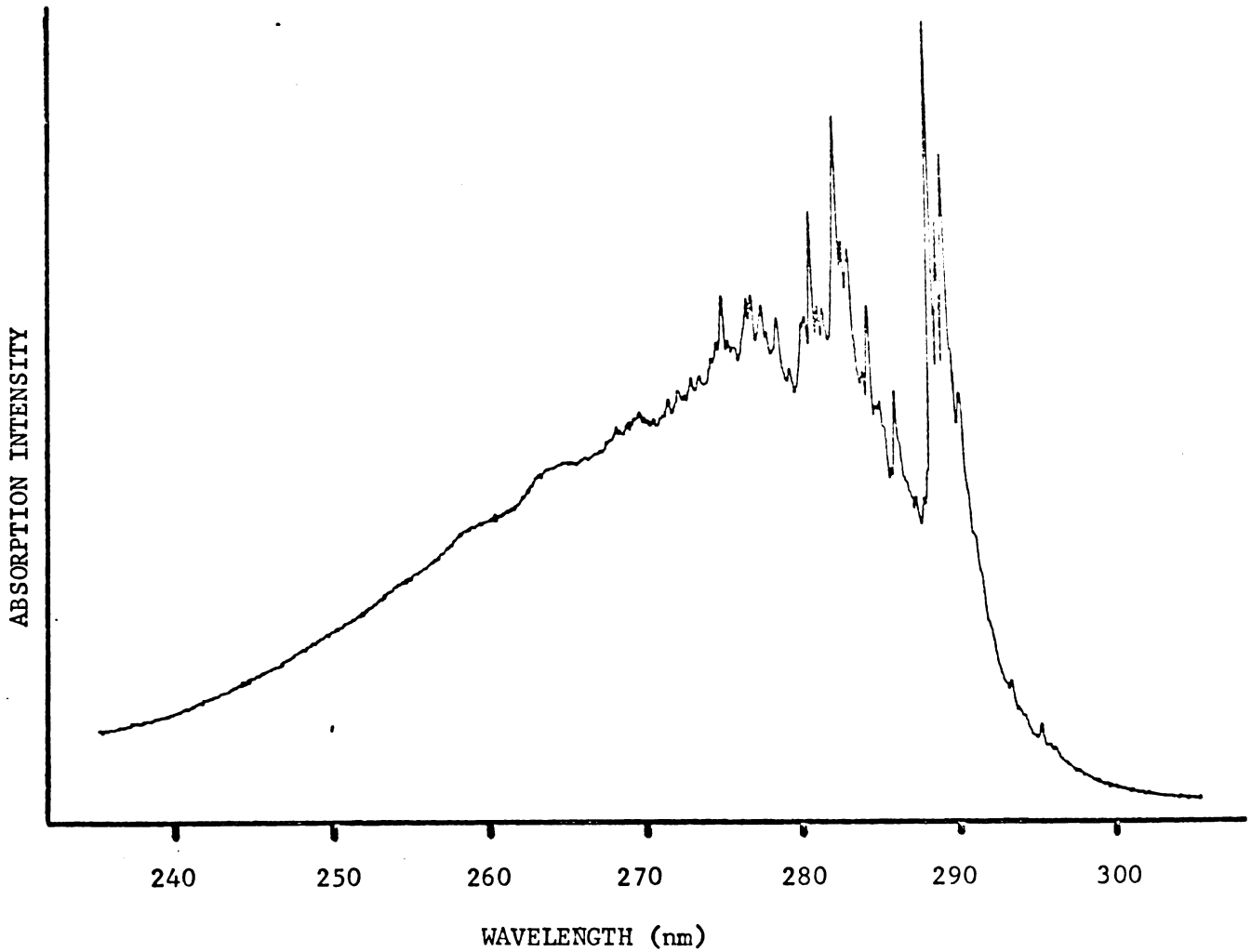

Figure 9. 7-Azaindole Vapor Absorption Spectrum.

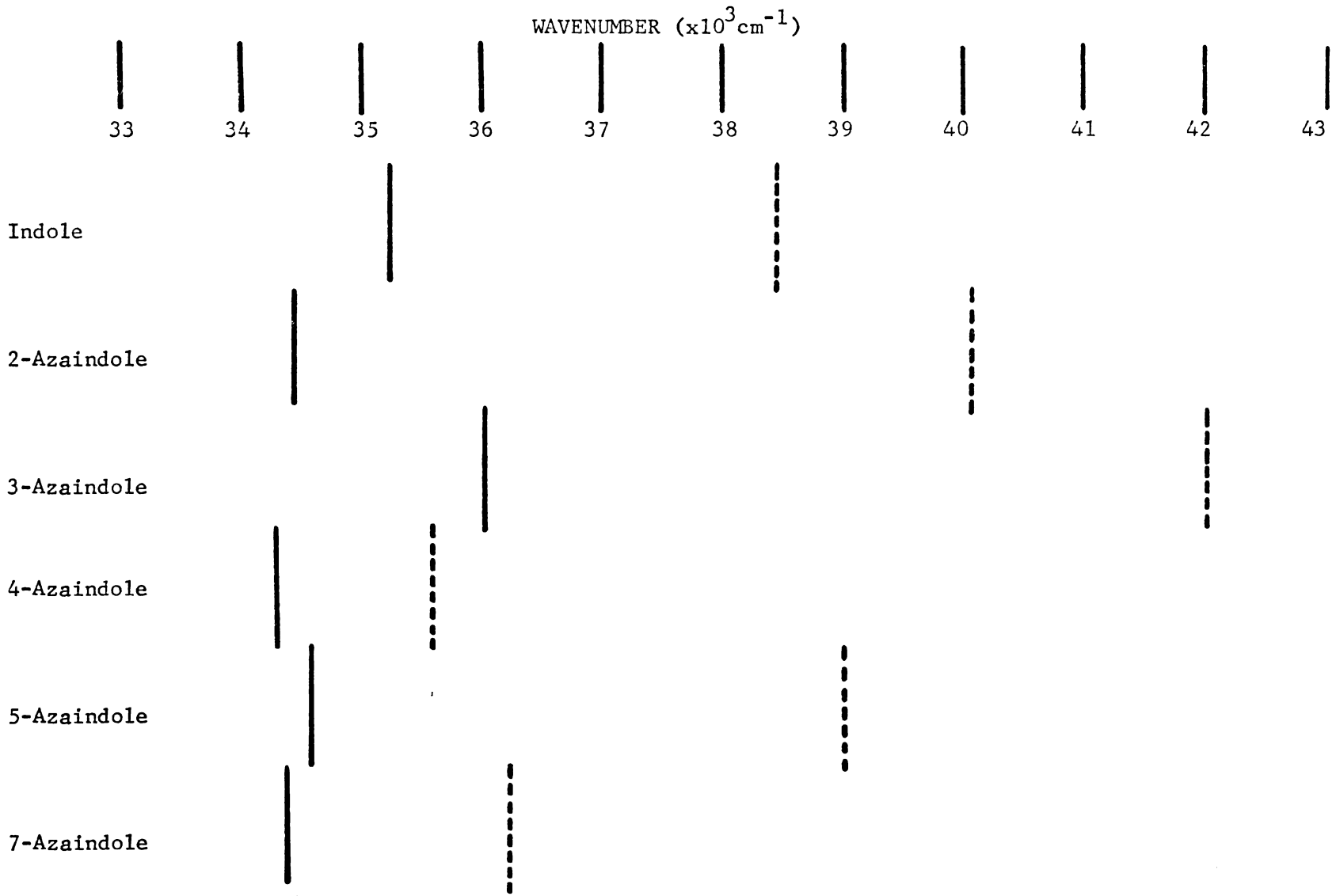

Table 1. ^1L_b(__) and ^1L_a(--) Absorption Band Energies of Indole and Azaindoles in the Vapor Phase.

Table 2. Experimental (Vapor) and Calculated Electronic State Energies of Indole and Azaindoles (in cm^{-1}, * maximum).

Compound	experimental ^1L_b 0-0	experimental ^1L_b (sequence)	calculated ^1L_b 0-0	experimental ^1L_a (sequence)	calculated ^1L_a 0-0
Indole	35229.8	35945.8 36670.0 37411.1	35457	38491.1* 39401.1	36912
2-Azaindole	34447.1	35186.4 35816.6 36536.3		39651.0 40783.0*	
3-Azaindole	36036	36791.7	36094	40983.6 42016.8*	37424
4-Azaindole	34399.7	35137	34788	35663.3*	36418
5-Azaindole	34626		35790	38022.8 38834.9 39082.5*	36914
6-Azaindole			35245		37374
7-Azaindole	34494.6	35335.6 36075.0	34955	36258.1* 37735.0 39215.6	36268

Figure 10. Calculated Charge Densities for Indole

10a. Numbers at each atomic position denote π -electron charge densities in electron units for ground state (top number), ^1L_a state (middle number), and ^1L_b state (bottom number).

10b. Numbers at each atomic position denote π -electron charge density differences from ground state (in electron units) for ^1L_a state (top number), and ^1L_b state (bottom number) with plus sign indicating an increase in electron density and minus sign indicating a decrease in electron density.

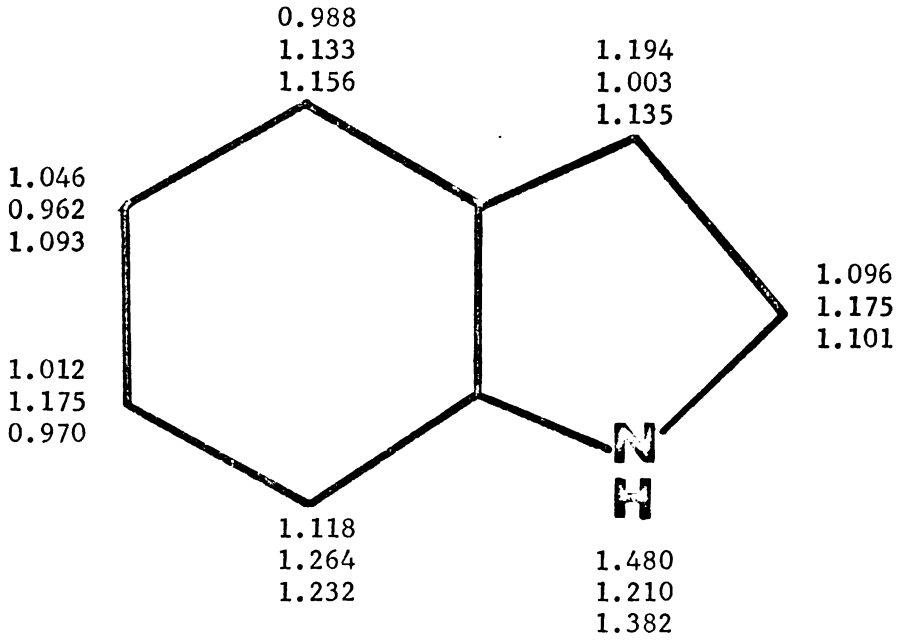

Figure 10a

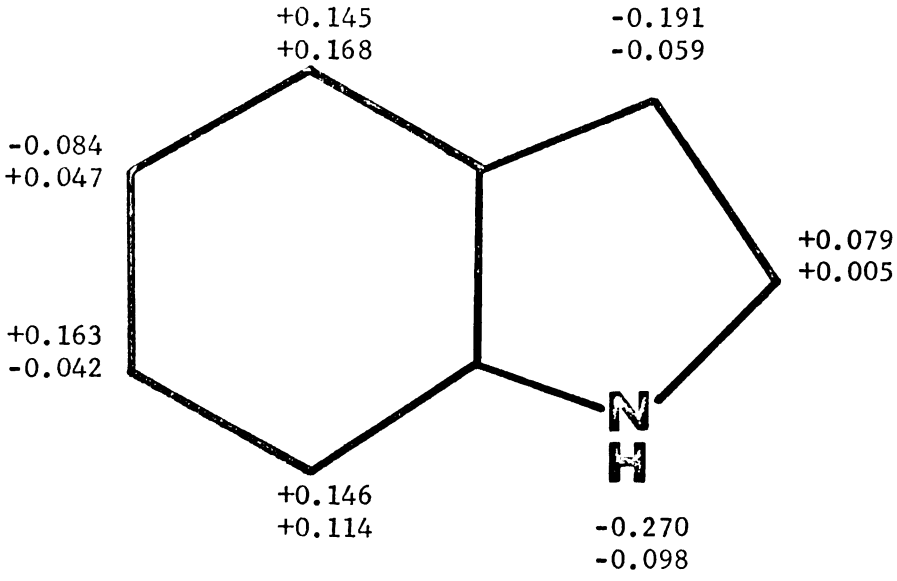

Figure 10b

CHAPTER 4

ABSORPTION SPECTRAL SHIFTS

-CORRELATION WITH EXCITED STATES CHARGE DENSITIES

Introduction

Vapor phase absorption spectra under reduced pressures represent spectra of essentially isolated molecules; high-resolution spectra show vibrational and rotational structures. The disappearance of rotational structure in vapor spectra due to high pressure and pressure broadening are manifestations of intermolecular interactions. In solution, the solute molecules are in contact or solvated by solvent molecules, this eliminates all rotational structures, and may cause blurring of vibration structure. At liquid nitrogen temperature (77°K), vibrational structure may become well resolved again.

Shifts due to solvent effects are often the result of several individual effects which may reinforce or cancel one another. They arise due to differences in interactions with the medium in the different electronic states. Interpretation should be related to the 0-0 band of an absorption or fluorescence spectrum; but it is often difficult to locate to 0-0 band in solution spectra. Therefore, shifts are usually referred to the maxima, which are not exactly affected the same way as 0-0 band.

Bayliss and McRae[11] pointed out that most solvent effects can be explained in terms of four main factors: (1) momentary transition dipole during optical absorption process (2) difference in the permanent dipole

moment between the ground and excited states of the solute (3) of Franck-Condon effects and (4) the dipole moment of the solvent. Solvent effects depend on various intermolecular interactions, such as dispersion forces, dipole-induced dipole, dipole-dipole, and hydrogen bonding. Dispersion forces are always operative in all solutions, whenever the solute and solvent are polar or not. This effect occurs when the transition dipole of the solute induces a momentary polarization in the solvent and is thus present in all solutions. Dipole-induced dipole and dipole-dipole interactions produce shifts in absorption spectra which may be to higher or lower energies. For non-polar solutes in non-polar or polar solvents, only dispersion forces are operative, which produced a moderate polarization red shift[12,13]. For polar solutes in non-polar solvents, dipole-induced dipole interactions take place, which produced either a red or a blue shift, depending on whether the excited state dipole moment of the solute increases or decreases. For polar solutes in polar solvents, dipole-dipole interactions can also cause a red or blue shift depending on whether the excited state dipole moment increases or decreases. In this case dipole-dipole interaction is the dominant cause for spectral shifts.

Franck-Condon principle plays a major role in solvent effects on both absorption and emission spectra. A solute molecule is surrounded by solvent molecules in equilibrium in solution. This equilibrium of ground state depends on (1) packing factor, which depend on geometry of the solvent and solute and (2) orientation factor, which depends on the mutual orientation interaction if the solute and solvent are polar or can form hydrogen bonding. The geometry, charge density and dipole moment of solute my be different in the excited state; therefore, the equilibrium configuration

of the solvent cage will also be different in the excited state. However, according to the Franck-Condon principle an optical transition occurs in a time (10^{-15}sec.) that is short compared with the period of nuclear motions. Therefore, the solvent configuration around the excited solute molecule, after this vertical transition, does not correspond to the equilibrium excited configuration, but to a conformation geometrically identical of the solvated ground state, i.e., a Franck-Condon state configuration. The orientation energy of this configuration is higher than that of the excited state equilibrium configuration, which can be reached by solvent relaxation of the system. The time required for geometrical rearrangement of solute is around 10^{-13}sec. and solvent reorientation around 10^{-11}sec. Since the lifetime of an excited singlet state is of the order of 10^{-9}sec., there is plenty of time for excited state equilibrium to be reached before deactivation occurs if the solvent is not viscous. Also the ground state configuration after fluorescence is not the equilibrium ground state configuration but a state of strain whose energy is higher than that of the ground state euqilibrium configuration (Figure 11).

The non-equilibrium configuration experiences two types of solvent strain upon solute molecules[11]. (1) packing strain and (2) orientation strain[14]. Packing strain results from an actual change in geometric size of the molecule in the excited and ground states. Generally the percentage change of the size of organic molecules is small and this strain can be neglected except in specific instances. The orientation strain results from the non-equilibrium orientation of the solvent cage around the solute molecule in its excited state and includes dipole-polarization and dipole-dipole interactions. Orientation strain is

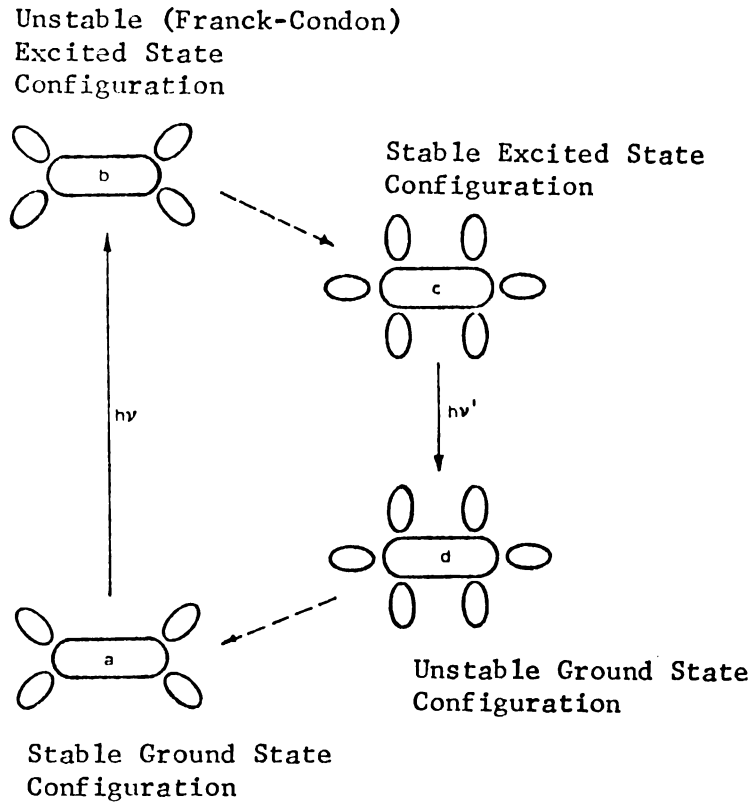

Figure 11. Illustrating Change of Solvation After Excitation or Emission

The large and small ovals representing solute and solvating solvent molecules are purely diagrammatic and are intended to represent a higher degree of solvation in the stable configuration of the excited state.

particularly important when solute and solvent are both polar and when the permanent dipole moment changes upon excitation. Modification of the strength of any hydrogen bonding would also give importance to this type of strain. If the dipole moment decreases in the excited state, the absorption undergoes a blue shift due to orientation strain, if the dipole moment increases in the excited state, this will cause a red shift. The fluorescence spectrum undergoes a red shift in both cases (Figure 12). Several studies have been made of the effect of hydrogen bonding on solvent shifts, that was first discussed by Kasha[7]. He pointed out that absorption bands corresponding the $\pi^* \leftarrow n$ transition blue shift in hydrogen bonding media. Later Brealey and Kasha[15] demonstrated that hydrogen bonding is the main influence in the $\pi^* \leftarrow n$ blue shift phenomenon in hydroxylic solvents. However, Pimentel[16] pointed out the dipole-induced dipole and dipole-dipole interaction produce small solvent shifts compared with those to hydrogen bonding. Pimentel discussed the influence of hydrogen bonding formation on electronic transition in terms of the Franck-Condon principle. In the case when hydrogen bonding is stronger in the ground state than the excited state (Figure 13a), the hydrogen bonding energy $W_e < W_g$, and the excitation energy implied by Franck-Condon principle is labeled w. But in the case when the hydrogen bonding is weaker in the ground state (Figure 13b), then $W_e > W_g$.

Solvent shifts due to hydrogen bonding can be formalized as follows:

$$\nu_a - \nu_o = \Delta\nu_a = W_g - W_e + w_e \qquad (8)$$

$$\nu_f - \nu_o = \Delta\nu_f = W_g - W_e - w_g \qquad (9)$$

When hydrogen bonding is stronger in the ground state $W_e < W_g$, so $\Delta\nu_a > 0$, i.e., a blue-shift which exceeds $W_g - W_e$ by w_e will be observed in absorption. Similarly the shift observed in emission, will be less than $W_g - W_e$

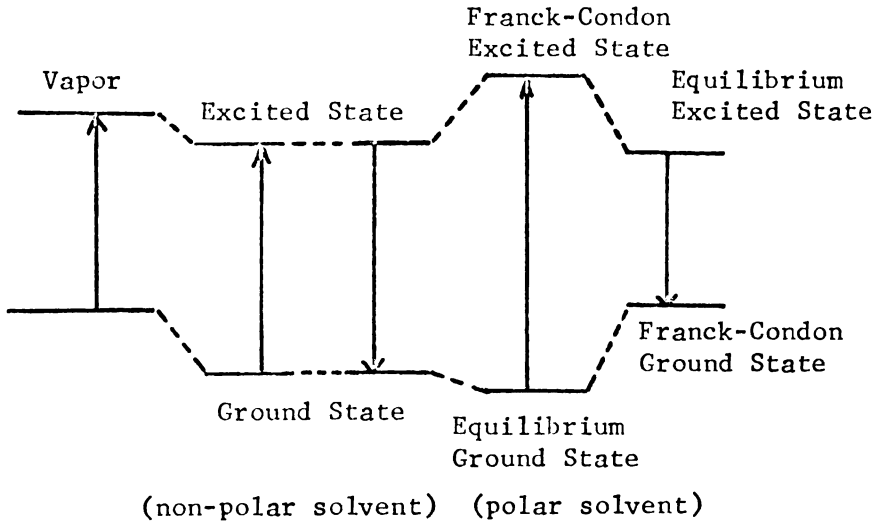

(i)

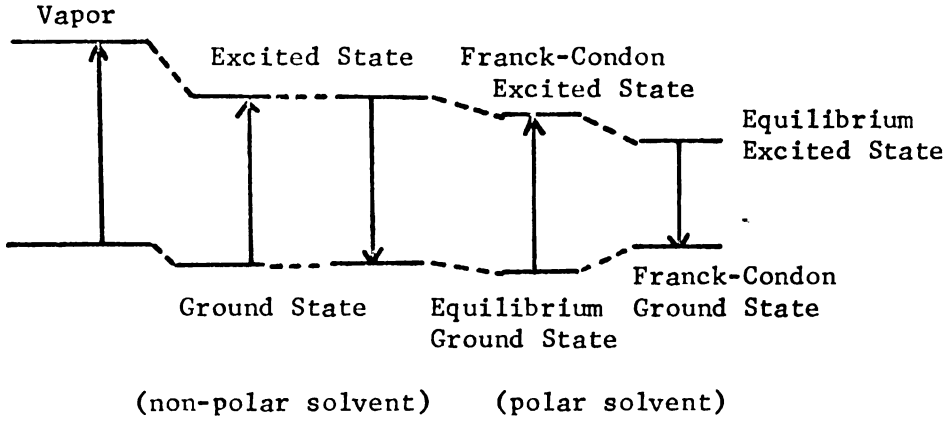

(ii)

Figure 12. Demonstration of solvent strain effects on energy levels of a polar solute in a polar solvent compared with a non-polar solvent and vapor. (i) Solute dipole moment decreases in the excited state; (ii) solute dipole moment increases in the excited state.

Figure 13. Solvent Shifts due to Hydrogen Bonding.

13a. Hydrogen Bonding Is Stronger in the Ground State

13b. Hydrogen Bonding Is Stronger in the Excited State

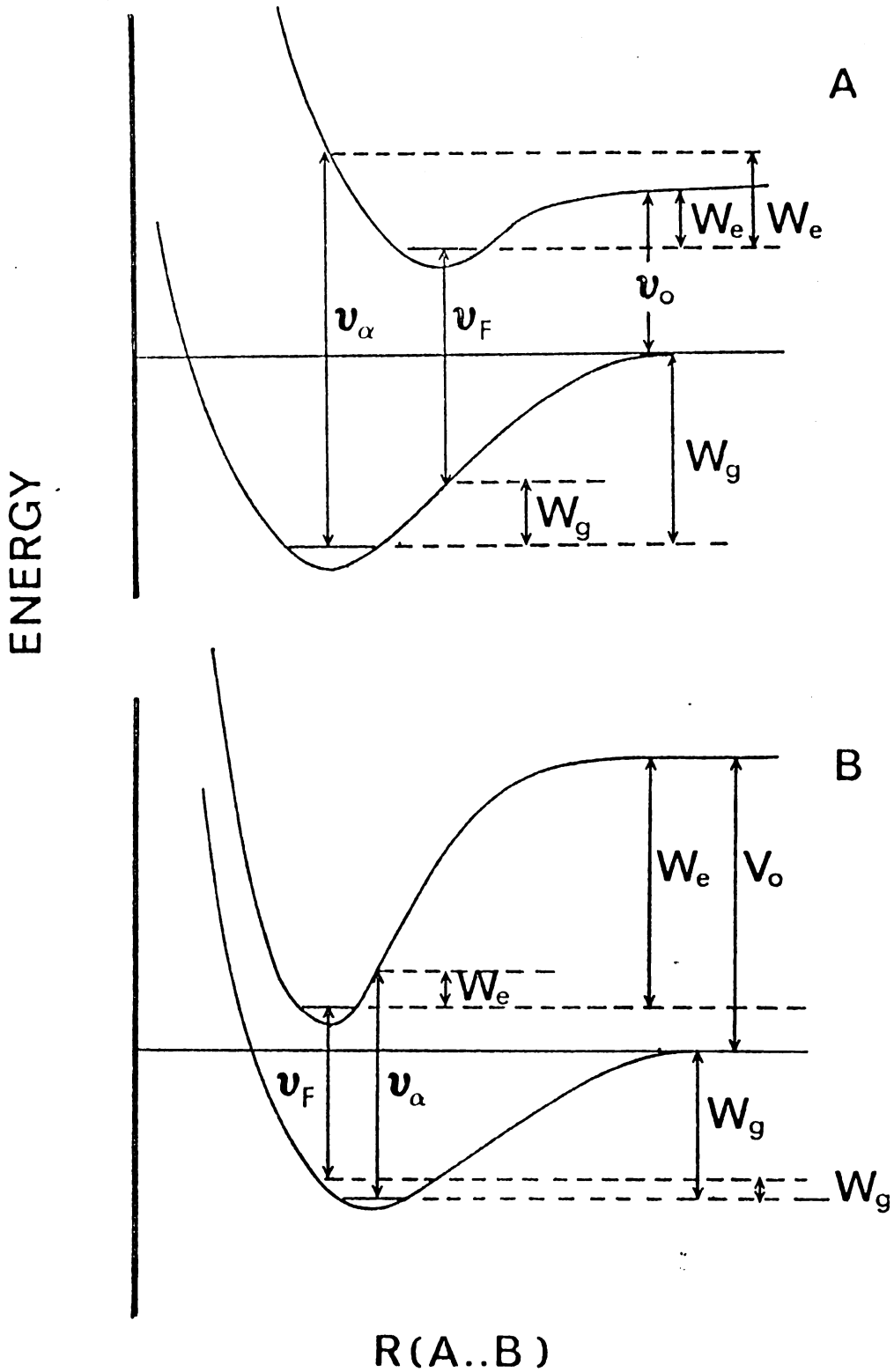
A
W_e
W_e
v_o
v_α
v_F
W_g
W_g
ENERGY
B
W_e
V_o
W_e
v_F
v_α
W_g
W_g
R(A..B)

by w_g and will be either a red or a blue shift depending on the specific case. When hydrogen bonding is weaker in the ground state $W_g < W_e$, both emission and absorption spectra will show a red shift. The well characterized hydrogen bonds have energies in the range of 1-7 kcal/mole (350-2500 cm^{-1}). According to the above discussion, a blue shift in absorption may exceed the ground state hydrogen bonding energy, hence, the expected blue shift occurs in the range of 350-2500 cm^{-1} or larger than 2500 cm^{-1}. But a red shift in absorption should never exceeds W_g, i.e., should not be larger than 2500 cm^{-1}. For $\pi^* \leftarrow n$ transition in hydrogen bonding media, a blue shift in absorption is usually observed. This is due to the decrease in charge density around the lone pair atom as a result of lone pair promotion. Thus, the hydrogen bond is always stronger in the ground state.

So a red shift in absorption spectrum indicated that the hydrogen bonding is stronger in the excited state[16]. This may indicate an increase in acidity or basisity depending on the functional group of the chromophore involved in hydrogen bonding.

As discussed above, when both solvent and solute are polar, electronic excitation to the Franck-Condon state is followed by a relaxation process, such that the solvent molecules rearrange themselves to the excited-equilibrium state. This kind of relaxation happens very fast at room temperature. But at very low temperature, the solvent forms rigid glass, and the solvent molecules are inhibited to relaxation process before emission occurs. In this case fluorescence occurs from a non-equilibrium Franck-Condon state or an intermediate state. Since Franck-Condon state is always higher in energy than the equilibrium excited state, fluorescence at liquid nitrogen temperature is blue shifted with respect to that in solution at room temperature.

Results and Discussions

The absorption spectra of indole and azaindoles were run in different media (3-methylpentane, diethyl ether, ethanol, water and dichloromethane). The purpose is to interpret spectral shifts in terms of the various possible interactions. These include: (1) dipole-dipole effects which reflect changes in the permanent dipole moment as a result of excitation (2) polarization shifts (3) hydrogen bonding (a) hydrogen bonding involving the pyrrolic hydrogen with the oxygen of ether, alcohol or water (b) hydrogen bonding involving the aza-nitrogen with the proton of alcohol or water (c) hydrogen bonding involving the pyrrolic nitrogen with the proton of alcohol or water. We analyzed the data by using 3-methylpentane (3MP) as a reference and the results are now discussed for each individual case.

Indole

Spectral shifts of indole in different media are shown in Table 3. In spite of the red shift observed in ether and ethanol solutions, a blue shift is observed in water. In hydrocarbon the shifts observed relative to vapor are attributed to general polarization red shifts as well as dipole-induced dipole interaction. The dipole moment of indole in the ground state is 2.3D and in the excited state 7.3D. Both types of interactions (i.e., dispersion and solute dipole-induced dipole interaction) should cause a red shift (Figure 12) compared with vapor spectra (Table 2). Our results show a red shift of -510 cm^{-1} and -897 cm^{-1} for ^1L_b and ^1L_a respectively.

In ether, besides the dispersion and dipole-induced dipole interaction, dipole-dipole interaction is taking place, because ether has a dipole moment of 1.3D[17]. In addition spectral shifts due to hydrogen bonding interaction between the pyrrolic hydrogen and ether lone pair oxygen must be taken into

Table 3. Absorption Spectral Shifts for Indole in Different Media.

Medium	^1L_b 0-0		$\Delta\bar{\nu}(cm^{-1})$	^1L_amax		$\Delta\bar{\nu}(cm^{-1})$
	λ(nm)	$\bar{\nu}(cm^{-1})$		λ(nm)	$\bar{\nu}(cm^{-1})$	
H_2O	286	34965	+122	269.5	37105	-489
EtOH	287.5	34782	- 61	271.5	36832	-762
Et_2O	288	34722	-121	271.5	36832	-762
CH_2Cl_2	288	34722	-121	271	36900	-694
3MP	287	34843	0	266	37594	0
Vapor	283.9	35223	+501	259.8	38491	+897

consideration. These effects should cause a further red shift if the pyrrolic hydrogen is more acidic in the excited state and because the excited state dipole moment is larger than the ground state dipole moment. Indeed, an additional red shift of -121 cm^{-1} and -762 cm^{-1} for ^1L_b and ^1L_a respectively, are observed due to change from 3MP to ether. In ethanol and water, an additional hydrogen bond can be formed involving the π - electron on the pyrrolic nitrogen and the lone pair oxygen of the solvent (Figure 14). If the nitrogen is less basic in the excited state, a blue shift will be expected. In alcohol the red shift is less than the observed in ether. Moreover a blue shift is observed in water. These results could only be interpreted in terms of a hydrogen bond involving the pyrrolic nitrogen which becomes weaker in the excited state. This indicated that the charge density on that nitrogen decreases upon excitation to ^1L_b or ^1L_a states.

Also for quantitative study of each of the shifts, absorption spectrum of indole in dichloromethane was taken (Table 3). Dichloromethane has a dipole moment of 1.5D[17] but can not form hydrogen bonds with indole. Spectral shifts in going from 3MP to CH_2Cl_2 can be useful in obtaining shifts that are solely due to dipole-dipole interaction $\Delta\nu_{d-d}$. Using Onsager's[19] formula

$$\Delta\nu_{d-d} = 2\mu_o(\mu_1 - \mu_o)\{(n^2-1)/2n^2+1) - (D-1)/(2D+1)\}/a^3hc \qquad (10)$$

where μ_o and μ_1 represent the dipole moment of the solute molecule in the ground and excited state, a is an effective cavity radius appropriate to the solvent, D is the dielectric constant of the solvent, n is the refractive index of solvent, one can therefore estimate shifts due to this effect in other polar solvent. The red shift due to dipole-dipole interaction in ether calculated by equation 10 is -92 cm^{-1} for ^1L_b band, which

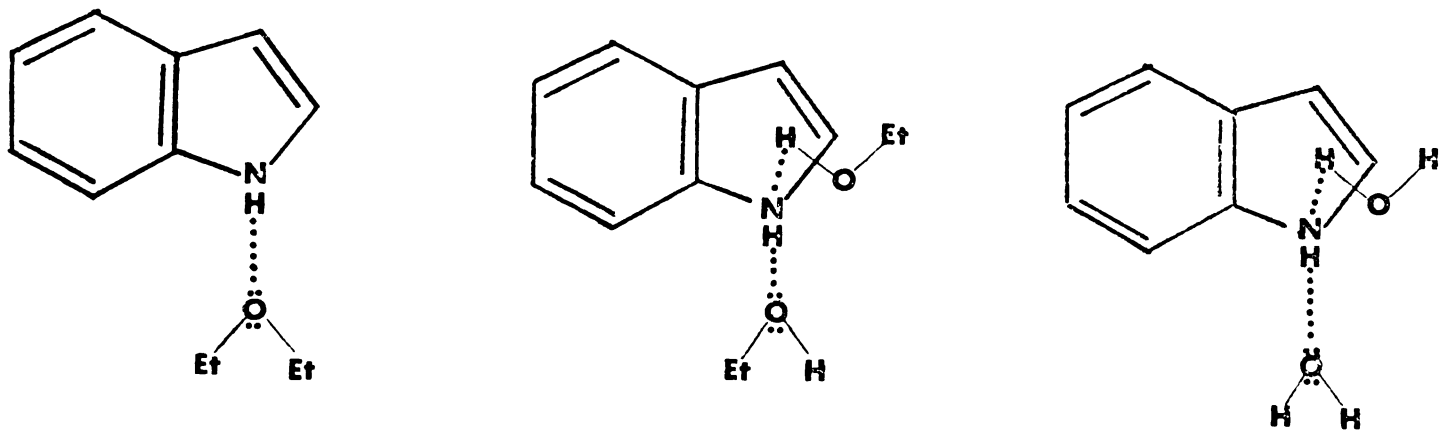

(i) (ii) (iii)

Figure 14. Hydrogen Bondings Between Indole and Solvents
(i) diethyl ether (ii) ethanol (iii) water.

indicates that a red shift of about -30cm^{-1} is due to hydrogen bonding effects for ^1L_b band. Similarly for the ^1L_a band, dipole-dipole red shift is -530 cm^{-1} and the hydrogen bonding red shift is -232 cm^{-1}.

From IR data[18], one may calculate the relative strengths of hydrogen bonding involving the oxygen lone pair of ethanol and water. Assuming the spectral shifts due to hydrogen bonding are proportional to the relative strength of hydrogen bonding in the ground state, one may estimate spectral shifts due to hydrogen bonding (>N-H····O) in ethanol and water (Table 4).

Charge density calculations using Pariser-Parr-Pople method was performed[10] to test these findings. The charge densities of indole in the ground, ^1L_b and ^1L_a states are shown in Figure 10a, and the charge density difference is shown in Figure 10b with plus sign indicating an increase in electron density and minus sign indicating a decrease in electron density. From Figure 10b, we noticed that charge density decreases at the pyrrolic nitrogen such decrease is more pronounced in the ^1L_a state compared to ^1L_b state. This implies an increase in the acidity of the pyrrolic hydrogen as a result of excitation to ^1L_b and particularly to ^1L_a state which will give rise to a red shift of the ^1L_b and ^1L_a bands. The magnitude of that shifts will be greater for ^1L_a band. The decrease in charge density at the pyrrolic nitrogen means that hydrogen bonding of the solvent proton with the pyrrolic nitrogen π -electron charge density is stronger in the ground state. This should cause a blue shift, specially the ^1L_a band. Since the acidity of water is about 100 times stronger than ethanol, we expect a much larger blue shift in water than ethanol due to this hydrogen bonding interaction. This explains the smaller magnitude of the red shift in ethanol and the change in sign of the shift (blue) observed in water.

Solvent effects on the absorption spectrum of indole lead to the

Table 4. Contributions of Dipole-Dipole Interaction and Hydrogen Bonding Interactions to the Observed Absorption Spectral Shifts for Indole.

State	Interactions	Et_2O	EtOH	H_2O
^1L_b	dipole-dipole	- 92	-159	-176
	>N-H·····O	- 30	- 27	- 24
	H-N<·····H	0	+121	+322
^1L_a	dipole-dipole	-530	-912	-1009
	>N-H·····O	-232	-209	-186
	H-N<·····H	0	+359	+706

following conclusions: (1) The permanent dipole moment of the ground (^1A), ^1L_b and ^1L_a state follows the order $^1L_a > {}^1L_b > {}^1A$. (2) The charge density at the pyrrolic nitrogen as calculated by Pariser-Parr-Pople method decreases in the excited states, which cause blue shifts due to hydrogen bonding involving the proton of the solvent particularly water, this is especially true for ^1L_a state. The calculated charge density change (Figure 10b) for the ^1L_a and ^1L_b states has a ratio of 2.7:1, and the blue shifts of ^1L_a and ^1L_b bands that are attributed to hydrogen bonding with the pyrrolic π -electron (H-N···H) have a ratio of 2.8:1 in ethanol and 2.3:1 in water. This is a good agreement and is not surprising inview of the fact that the energy of the hydrogen bond involving the pyrrolic nitrogen reflects directly the π-charge density at that site. (3) The decrease in charge density at the pyrrolic nitrogen due to excitation causes the pyrrolic hydrogen to be more acidic in the excited states particularly the ^1L_a. This causes red shifts but quantitative correlation is not expected since the acidity of the hydrogen does not reflect quantitative changes in charge density at the pyrrolic nitrogen.

Azaindoles

Absorption spectra of 2-, 3-, 4-, 5-, and 7-azaindoles have been taken in water, ethanol, ether, dichloromethane and 3-methylpentane. Spectral shift data are presented in Table 5 and are interpreted in a similar way as indole but also taking into consideration the fact the azanitrogen forms hydrogen bonds with protic solvents (Table 6).

Spectral red shifts in hydrocarbon with respect to the vapor reflect an increase in the excited state permanent dipole moment particularly in the ^1L_a state. After attributing spectral shifts to the various interactions (Table 6), we conclude that in the case of 2-azaindole there is a

Table 5. Absorption Spectral Shifts for Azaindoles in Different Media.

Compound	Medium	^1L_b 0-0 λ(nm)	^1L_b 0-0 $\bar{\nu}$(cm^{-1})	$\Delta\bar{\nu}$(cm^{-1})	^1L_a max λ(nm)	^1L_a max $\bar{\nu}$(cm^{-1})	$\Delta\bar{\nu}$(cm^{-1})
2-Azaindole	H_2O	296	33783	-230	250.5	39920	-160
	EtOH	296.5	33727	-286	252	39682	-398
	Et_2O	296	33783	-230	252	39682	-398
	CH_2Cl_2	296	33783	-230	252	39682	-398
	3MP	294	34013	0	249.5	40080	0
	Vapor	290.3	34447	+434	245.3	40766	+686
3-Azaindole	H_2O	277.5	36036	+376	243	41152	- 85
	EtOH	279.5	35778	+128	244.5	40899	-388
	Et_2O	281	35587	- 63	243	41152	- 85
	CH_2Cl_2	281	35587	- 63			
	3MP	280.5	35650	0	242.5	41237	0
	Vapor	277	36101	+451	238	42016	+779
4-Azaindole	H_2O				289.5	34542	-607
	EtOH				288	34722	-427
	Et_2O				288	34722	-427
	CH_2Cl_2				288	34722	-427
	3MP	296	33783	0	284.5	35149	0
	Vapor	290.8	34387	+604	280.4	35663	+514
5-Azaindole	H_2O				264.5	37807	-877
	EtOH				265	37664	-949
	Et_2O				263	38022	-662
	CH_2Cl_2				263	38022	-662
	3MP				258.5	38684	0
	Vapor				252	39682	+998
7-Azaindole	H_2O				289	34602	-241
	EtOH				290	34482	-361
	Et_2O				288	34722	-121
	CH_2Cl_2				288	34722	-121
	3MP	294	34013	0	287	34843	0
	Vapor	288.8	34626	+613	277.5	36036	+1193

Table 6. Contributions of Dipole-Dipole Interaction and Hydrogen Bonding Interactions to the Observed Absorption Spectral Shifts for Azaindoles (in cm^{-1}).

Compound	State	Interactions	Et_2O	EtOH	H_2O
2-Azaindole	^1L_b	Dipole-Dipole	-176	-302	-335
		>N-H·····O	- 54	- 45	- 34
		H-N·····H	0	+ 61	+139
		+=N:·····H			
	^1L_a	Dipole-Dipole	-303	-539	-579
		>N-H·····O	- 77	- 69	- 61
		H-N·····H	0	+218	+480
		+=N:·····H			
3-Azaindole	^1L_b	Dipole-Dipole	- 48	- 83	- 92
		>N-H·····O	- 15	- 12	- 9
		H-N·····H	0	+223	+477
		+=N:·····H			
4-Azaindole	^1L_a	Dipole-Dipole	-372	-640	-708
		>N-H·····O	- 55	- 45	- 36
		H-N·····H	0	+258	+137
		+=N:·····H			
5-Azaindole	^1L_a	Dipole-Dipole	-505	-870	-962
		>N-H·····O	-156	-128	-100
		H-N·····H	0	+ 49	+185
		+=N:·····H			
7-Azaindole	^1L_a	Dipole-Dipole	- 92	-159	-176
		>N-H·····O	- 29	- 24	- 18
		H-N·····H	0	-179	- 47
		+=N:·····H			

possibility that the charge density on the azanitrogen increases, leading to a stronger hydrogen bond of the type >N:···H in the excited state. (The Pariser-Parr-Pople calculation for 2-azaindole is not available because of the adjacent nitrogens). This causes a red shift and will therefore reduce the blue shift associated with hydrogen bonding with the pyrrolic nitrogen (H-N····H). For 3-azaindole, the hydrogen bonding effect caused quite a blue shift which indicated that the π -electron charge density for both pyridinic and pyrrolic nitrogen decreassed in the excited state. This is consistent with the charge density calculated by Pariser-Parr-Pople method (Figure 15). The reason for smaller dipole-dipole interaction in the case of 3-azaindole compared to other azaindoles reflects the smaller changes in the permanent dipole moment upon excitation. In 4-azaindole only ^1L_a state is available because the ^1L_b band is completely submerged. Hydrogen bonding effect involving the pyrrolic nitrogen is smaller compared with indole. This can be explained as an increase in shifts due to hydrogen bonding with the azanitrogen which reduces the blue shift caused by interaction with the pyrrolic nitrogen. This is also consistent with charge density calculation (Figure 16). Same arguement has been applied to 5-, and 7-azaindole spectral shifts which are also consistent with charge density calculation (Figure 17 and 18). In the case of 7-azaindole, hydrogen bonding is fully dominated by the spectral red shift due to hydrogen bonding involving the azanitrogen.

Solvent effects on the absorption spectra of azaindoles lead to the following conclusions: (1) The ^1L_a and ^1L_b state permanent dipole moment are larger than the ground state permanent dipole moment, with ^1L_a larger than the ^1L_b state. (2) The charge density at the pyrrolic nitrogen decreases in the excited state which gives rise to a blue shift in hydrogen

Figure 15. Calculated Charge Densities for 3-Azaindole.

15a. Numbers at each atomic position denote π -electron charge densities in electron units for ground state (top number), ^1L_b state (middle number), and ^1L_a state (bottom number).

15b. Numbers at each atomic position denote π -electron charge density defferences from ground state (in electron units) for ^1L_b (top number), and ^1L_a state (bottom number) with plus sign indicating an increase in electron density and minus sign indicating a decrease in electron density.

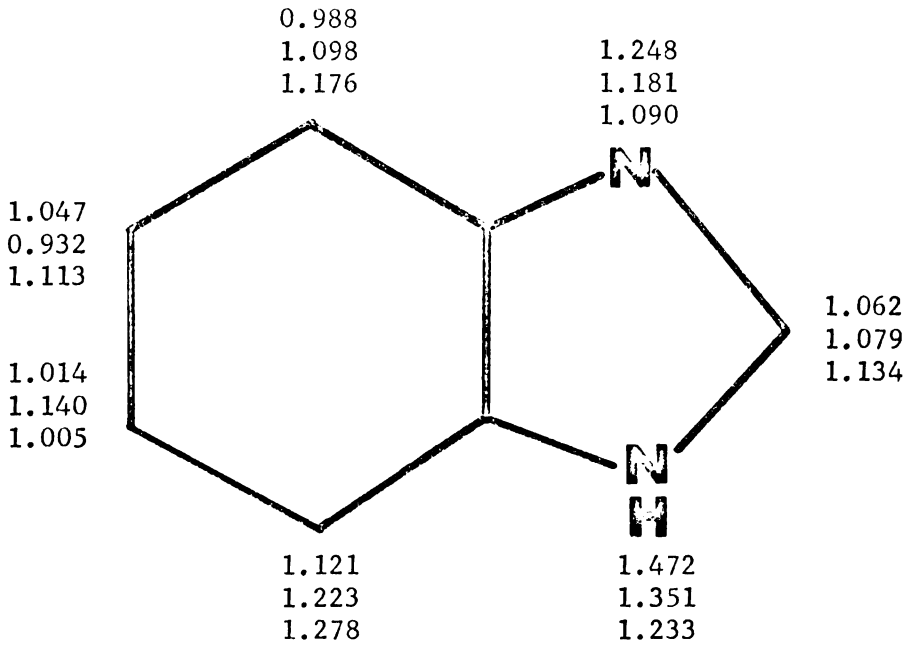

Figure 15a

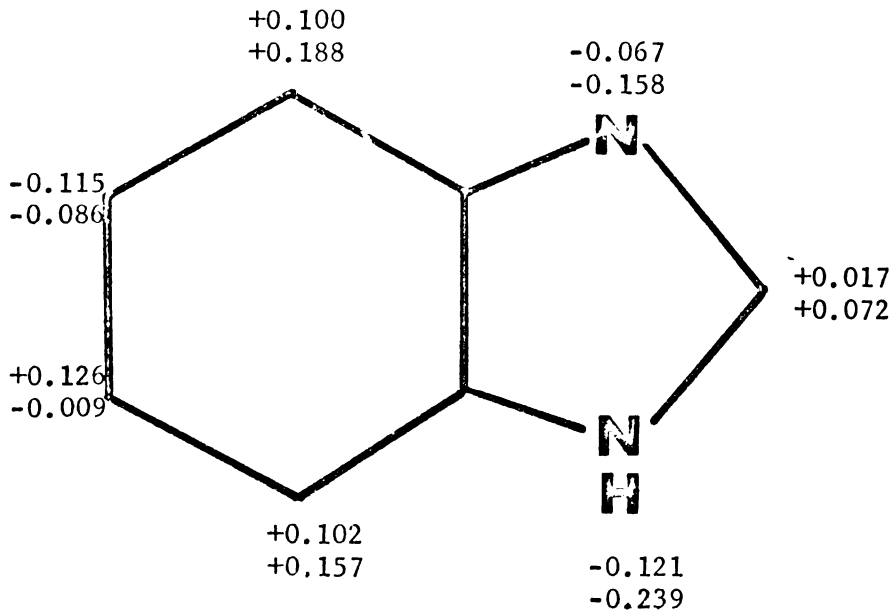

Figure 15b

Figure 16. Calculated Charge Densities for 4-Azaindole.

16a. Numbers at each atomic position denote π -electron charge densities in electron units for ground state (top number), ^1L_b state (middle number), and ^1L_a state (bottom number).

16b. Numbers at each atomic position denote π -electron charge density differences from ground state (in electron units) for ^1L_b state (top number), and ^1L_a state (bottom number) with plus sign indicating an increase in electron density and minus sign indicating a decrease in electron density.

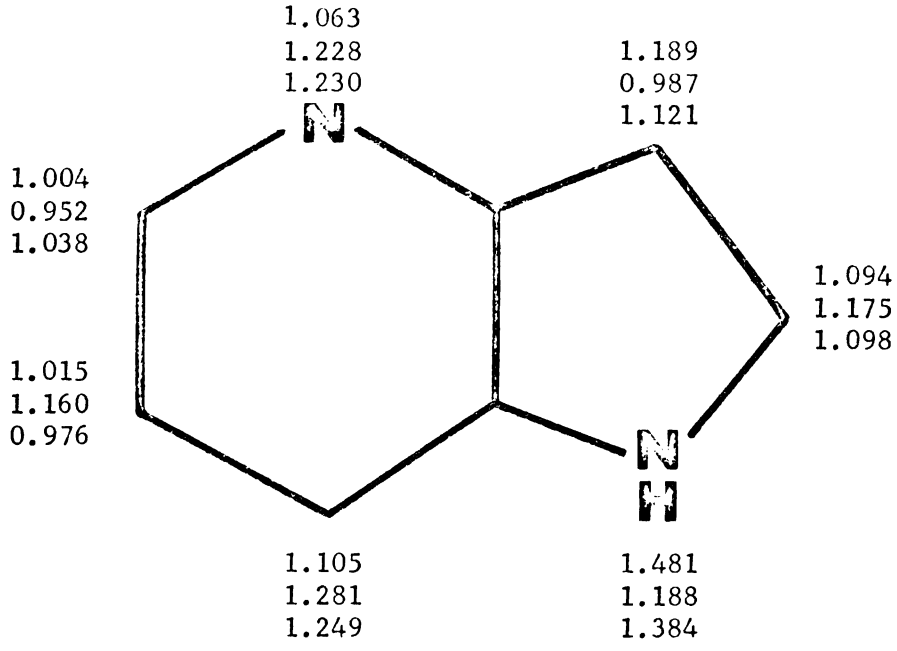

Figure 16a

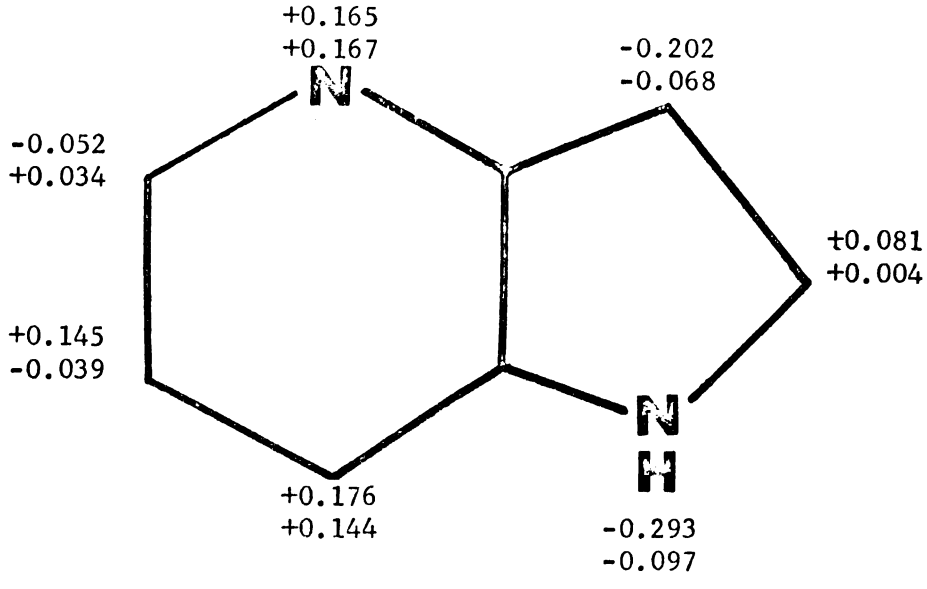

Figure 16b

Figure 17. Calculated Charge Densities for 5-Azaindole.

17a. Numbers at each atomic position denote π -electron charge densities in electron units for ground state (top number), ^1L_b state (middle number), and ^1L_a state (bottom number).

17b. Numbers at each atomic position denote π -electron charge density differences from ground state (in electron units) for ^1L_b state (top number), and ^1L_a state (bottom number) with plus sign indicating an increase in electron density and minus sign indicating a decrease in electron density.

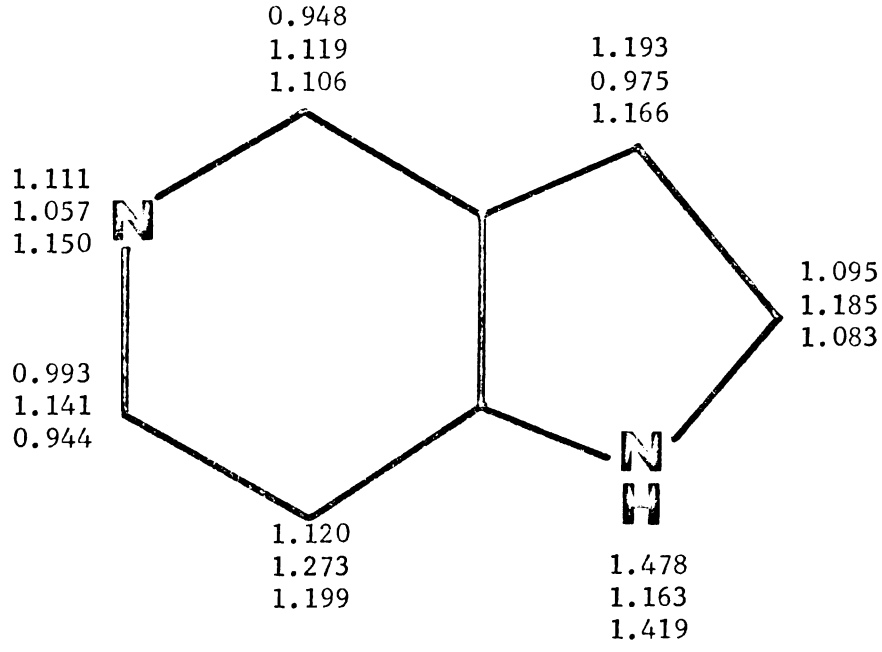

Figure 17a

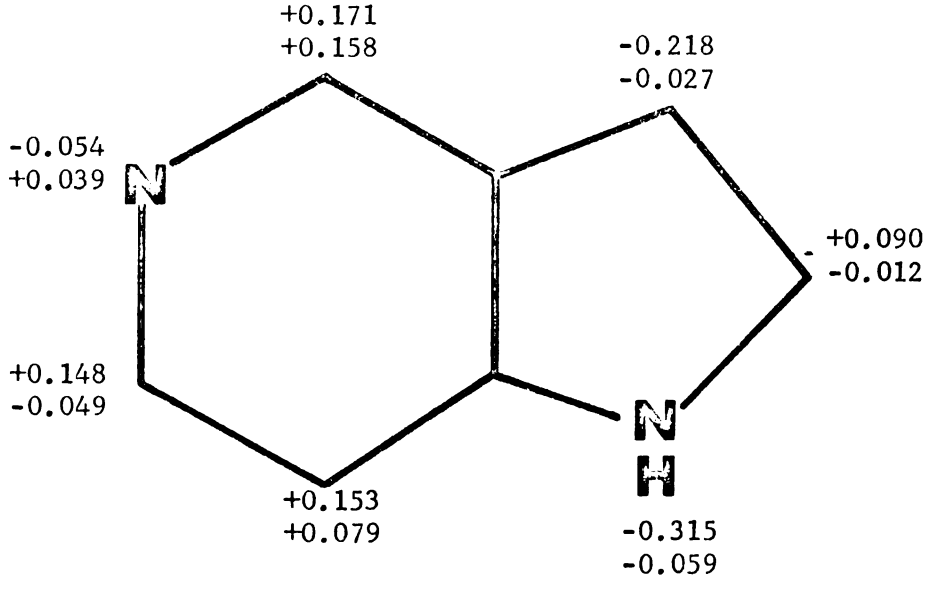

Figure 17b

Figure 18. Calculated Charge Densities for 7-Azaindole.

18a. Numbers at each atomic position denote π -electron charge densities in electron units for ground state (top number), ^1L_b state (middle number), and ^1L_a state (bottom number).

18b. Numbers at each atomic position denote π -electron charge density differences from ground state (in electron units) for ^1L_b state (top number), and ^1L_a state (bottom number) with plus sign indicating an increase in electron density and minus sign indicating a decrease in electron density.

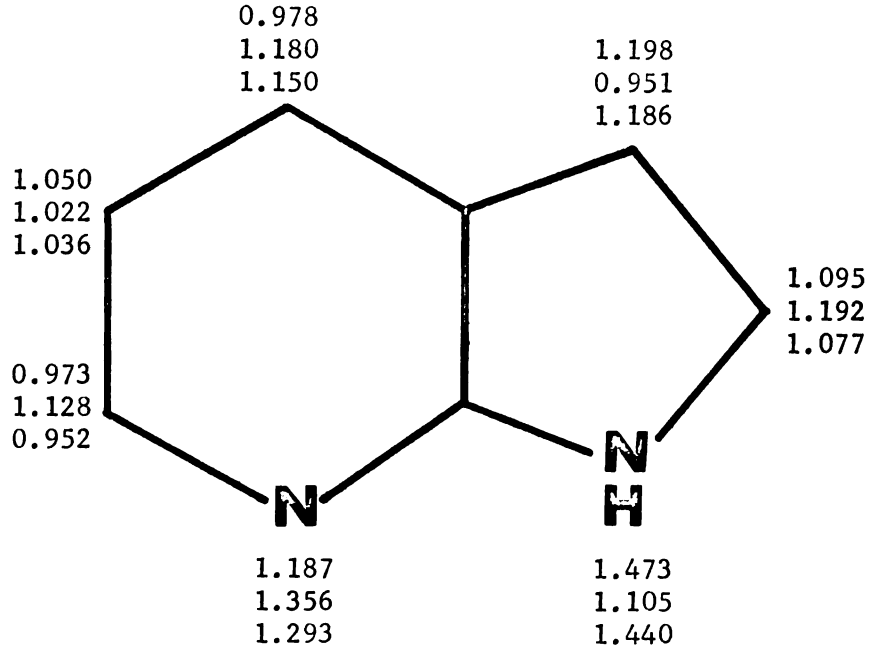

Figure 18a

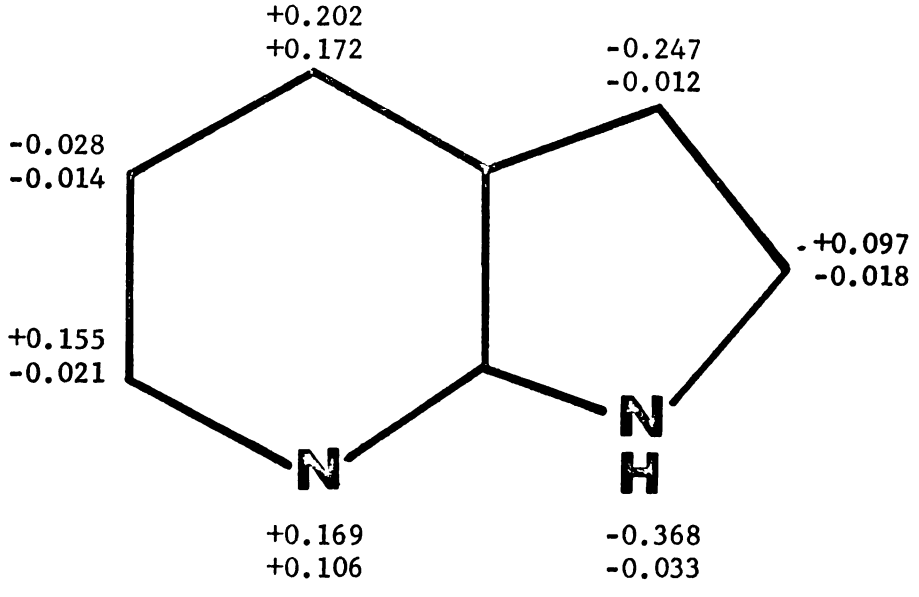

Figure 18b

bonding solvents. (3) The pyrrolic hydrogen is more acidic in the excited state than the ground state, this causes a red shift. (4) The charge density at the pyridinic nitrogen decreased in 3-azaindole but increase in 4-, 5-, and 7-azaindoles, which causes a blue and red shift respectively. The shift due to this effect may be large enough to govern the observed spectral shift.

CHAPTER 5

EMISSION SPECTRA OF INDOLE AND AZAINDOLES

Introduction

Our interest here is to study the solvent effect on emission spectra and to obtain values for excited state dipole moment and excited state pK's for indole and azaindoles. The emission characteristics of a molecule in different solvents is governed by (1) the influence of the dielectric properties of the solvent on the excited state of the solute (2) hydrogen bonding between solvent and solute in the excited state (3) solvent relaxation during the lifetime of the solute's excited state.

Idealy, it would be expected that the 0-0 absorption and emission bands would coincide since the energy change is identical. But this is not usually the case. If the solvent and solute are both nonpolar, or one is polar, the frequency shifts in 0-0 absorption and emission bands are predicted to be the same or nearly the same. Therefore the 0-0 bands should be coincide or nearly so (Figure 12). In these cases, dispersion and dipole induced dipole terms are the principal contributing factors to solvent-solute interaction and the orientation strain is negligible leading to no or very little difference in energy between the Franck-Condon state and the equilibrium state. Thus the state that is reached by absorption and that from which emission originates are nearly the same.

When the solute and solvent are both polar, and there is negligible

change in the dipole moment as a result of excitation, the frequency shift for fluorescence is the same as that for absorption, again the 0-0 bands in the absorption and emission processes should be the same or nearly so.

If the dipole moment of the solute changes (in magnitude and/or direction) upon excitation and the solvent is polar, reorientation may occur before emission. However, if the solvent is rigid, relaxation times are several order magnitude larger than the excited state lifetime, so emission occurs before solvent rearrangement takes place. If however the polar solvent is fluid, relaxation is much more rapid emission may occur from the equilibrium excited state where dipole reorientation is completed. Therefore, absorption will occur to the metastable Franck-Condon state ($\bar{\nu}_{abs}$), emission will occur from the equilibrium state ($\bar{\nu}_{emiss}$). The quantitative expression for the $\Delta\bar{\nu}$ in absorption is different from that in emission and the 0-0 bands will not coincide. The difference (Stokes shift) is:

$$\Delta\bar{\nu}_{a-f} = \nu_{abs} - \nu_{emiss} = 2(\mu_e - \mu_g)^2\{(D-1)/(D+2) - (n^2-1)/(n^2+2)\}/a^3hc \quad (11)$$
$$+ 2\{(\alpha_e - \alpha_g)(3\mu_g^2 - 5\mu_e^2 + 2\mu_g\mu_e)\}\{(D-1)/(D+2) - (n^2-1)/(n^2+2)\}^2/a^6hc$$

where μ_g and μ_e represent the dipole moment of the solute molecule in the ground and excited state, a is an effective cavity radius appropriate to the solvent, D is the dielectric constant of the solvent, n is the refractive index of solvent, and α_g and α_e are the polarizabilities of the solute molecule in the ground and excited states.

The second term originates from the dipole-induced dipole interaction, in many cases can be consider as a second order interaction term and makes a negligible contribution to the shift, and the equation is simplified as

follows:

$$\Delta\bar{\nu}_{a-f} = \nu_{abs} - \nu_{emiss} = 2(\mu_e - \mu_g)^2\{(D-1)/(D+2) - (n^2-1)/(n^2+2)\}/a^3hc \quad (12)$$

The dipole moment difference in ground and excited state can be obtained directly from the Stokes shift. An estimate of the excited state dipole can be made from experimental absorption and emission shift data and the known ground state dipole moment using equation 12.

Another interesting consideration is the effect of electronic excitation on the pK_a of certain compounds in the excited state compared with the ground state. This is of special interest to us in relation to the phenomenon of proton-transfer in the excited state. Weller[20,21,22] has discussed methods of determing the excited singlet-state dissociation constant, pK*, from spectroscopic data. The determination of $\Delta pK = (pK - pK^*)$ of this system is based on the energy diagram shown in Figure 19 and the thermodynamic quantities from the equilibria:

$$X\text{-}H\cdots\cdots Y \rightleftarrows X^-\cdots\cdots H^+\text{-}Y \quad (13)$$

$$X\text{-}H^*\cdots\cdots Y \rightleftarrows X^{-*}\cdots\cdots H^+\text{-}Y \quad (14)$$

From the diagram in Figure 19, we get:

$$\Delta E + E_d^* = \Delta E' + E_d \quad (15)$$

where ΔE and $\Delta E'$ are the energy changes for the transition from the ground electronic state to the lowest-excited singlet state of the proton donor and acceptor, respectively. The dissociation energies in the ground and excited states, E_d and E_d^*, can be written

$$E_d - E_d^* = (\Delta G - T\Delta S) - (\Delta G^* - T\Delta S^*) \quad (16)$$

Assuming $\Delta S = \Delta S^*$, then

$$\Delta G - \Delta G^* = -RT(\ln K - \ln K^*) = E_d - E_d^*$$

$$= \Delta E - \Delta E' \quad (17)$$

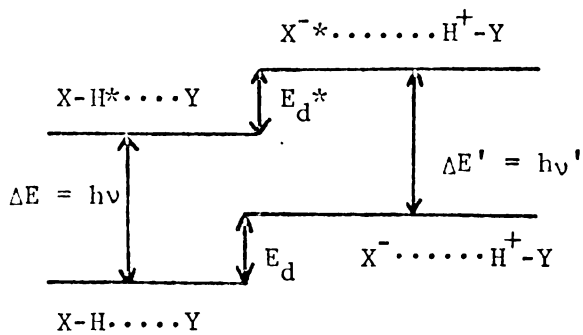

Figure 19. Schematic Thermochemical Diagram for Determination of Excited-State pK_a Values.

Since $\log K = -pK$,

$$pK - pK^* = (\Delta E - \Delta E')/2.303RT \quad (18)$$

where the energy changes ΔE and $\Delta E'$ can be estimated from the frequencies measured at the maxima of absorption and fluorescence by means of

$$\Delta E = h\nu = (h\nu_A + h\nu_F)/2 \quad (19)$$

$$\Delta E' = h\nu' = (h\nu_A' + h\nu_F')/2 \quad (20)$$

Results and Discussions

Solvent Effects on Luminescence Spectra

Emission spectra of indole and 2-, 3-, 4-, 5-, and 7-azaindoles were determined at room temperature and at 77°K in dilute solution of 3MP, ether, ethanol, water and acidic and basic media (Table 7 and Figures 20-21). A considerable red shift in room temperature fluorescence spectra is observed in all compounds when the medium is changed from non-polar to polar solvent. Such red shift is due to solvent relaxation during the excited state lifetime from the metastable Franck-Condon state to an equilibrium excited state before fluorescence occurs. The low temperature fluorescence spectra establishes clearly that the emission do not arise from the equilibrium state but from essentially the Franck-Condon state, the shifts shown, correspond to those observed in the absorption spectra. The low temperature phosphorescence data and lifetimes are also shown in Table 7. The charge distributions and pK's of the triplet states are not expected to changed dramatically as in the first excited singlet state, we expect therefore that the triplet states to have properties closer to those of the ground state. The energies of the phosphorescence peaks in different solvents are close to each other, but the phosphorescence lifetimes are usually longer in the polar solvents. In Table 7, we notice that for 7-azaindole in 3MP and ethanol, two luminescence bands are observed at

Table 7. Fluorescence (F) and Phosphorescence (P) Spectra of Indole and Azaindoles in Different Media (in nm).

Compound	Solvent	$\lambda_{F_{max}}$ (R.T.)[1]	$\lambda_{F_{max}}$ (77°K)	$\lambda_{P_{max}}$	τ_P (sec.)
Indole	H_2O	350			
	(low pH)	Q[2]			
	(high pH)	Q			
	EtOH	339	314	433	6.7
	Et_2O	326	320	440	6.8
	3MP	310	314	440	2.8
2-Azaindole	H_2O	328			
	(low pH)	375			
	(high pH)	377			
	EtOH	328	319	454	3.9
	Et_2O	326	325	460	4.3
	3MP	318	314	448	3.7
3-Azaindole	H_2O	303			
	(low pH)	380			
	(high pH)	Q			
	EtOH	305	295	425	5.7
	Et_2O	302	302	422	5.2
	3MP	304	292	420	3.6
4-Azaindole	H_2O	432			
	(low pH)	Q			
	(high pH)	Q			
	EtOH	378	368	435	2.4
	Et_2O	352	350	422	2.0
	3MP	328	285		

Table 7 (cont'd.).

Compound	Solvent	$\lambda_{F_{max}}$ (R.T.)[1]	$\lambda_{F_{max}}$ (77°K)	$\lambda_{P_{max}}$	τ_P(sec.)
5-Azaindole	H_2O	415			
	(low pH)	Q			
	(high pH)	Q			
	EtOH	356	336	442	4.0
	Et_2O	345	330	450	3.7
	3MP	295	295	440	1.1
7-Azaindole	H_2O	395			
	(low pH)	425			
	(high pH)	Q			
	EtOH	372 (500)[3]	350	452	3.1
	Et_2O	346	344	460	3.0
	3MP	324 (480)[3]	360	472	1.1

1. Room Temperature
2. Quenched
3. F_2

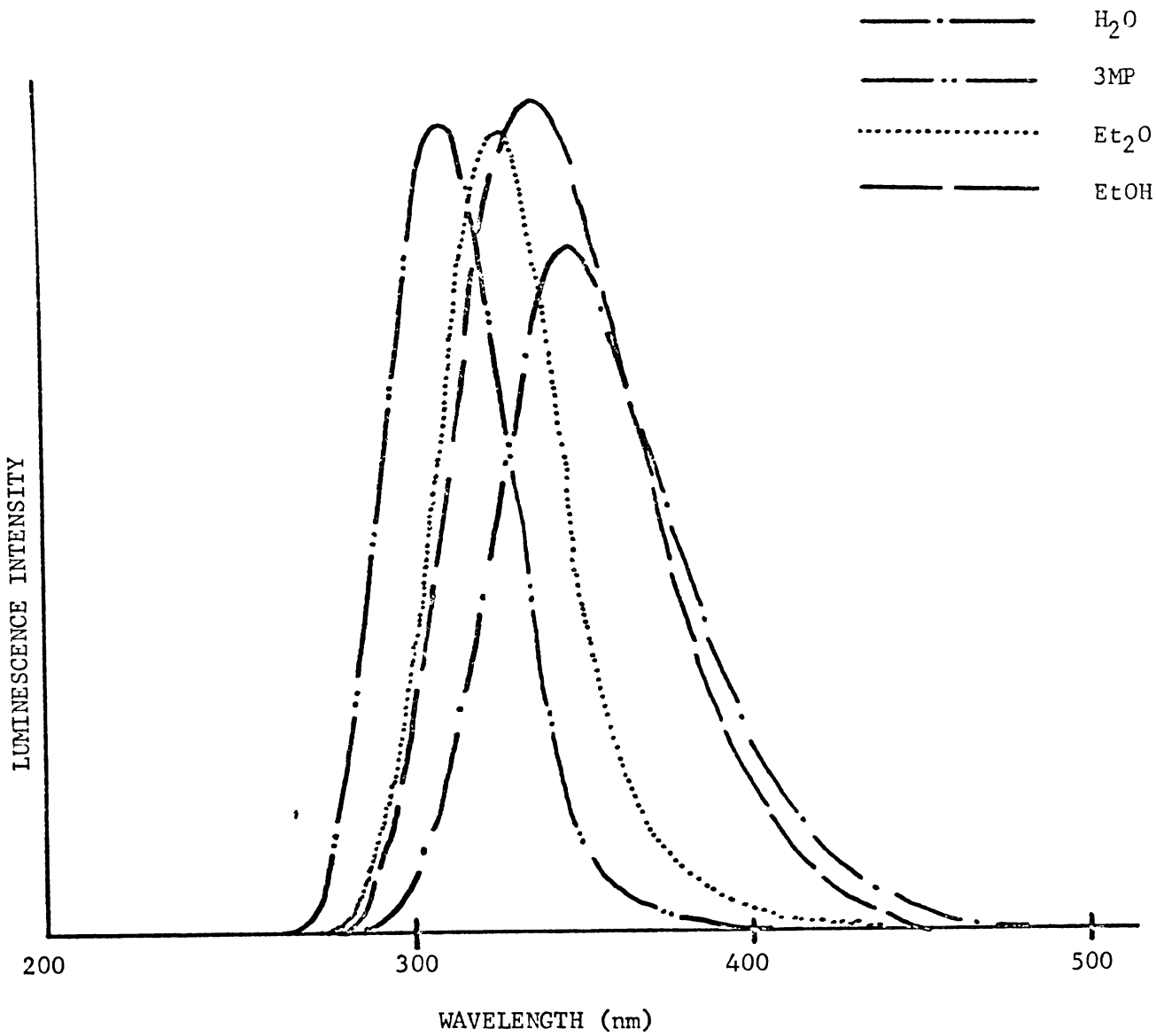

Figure 20. Emission Spectra of Indole in Different Media at Room Temperature.

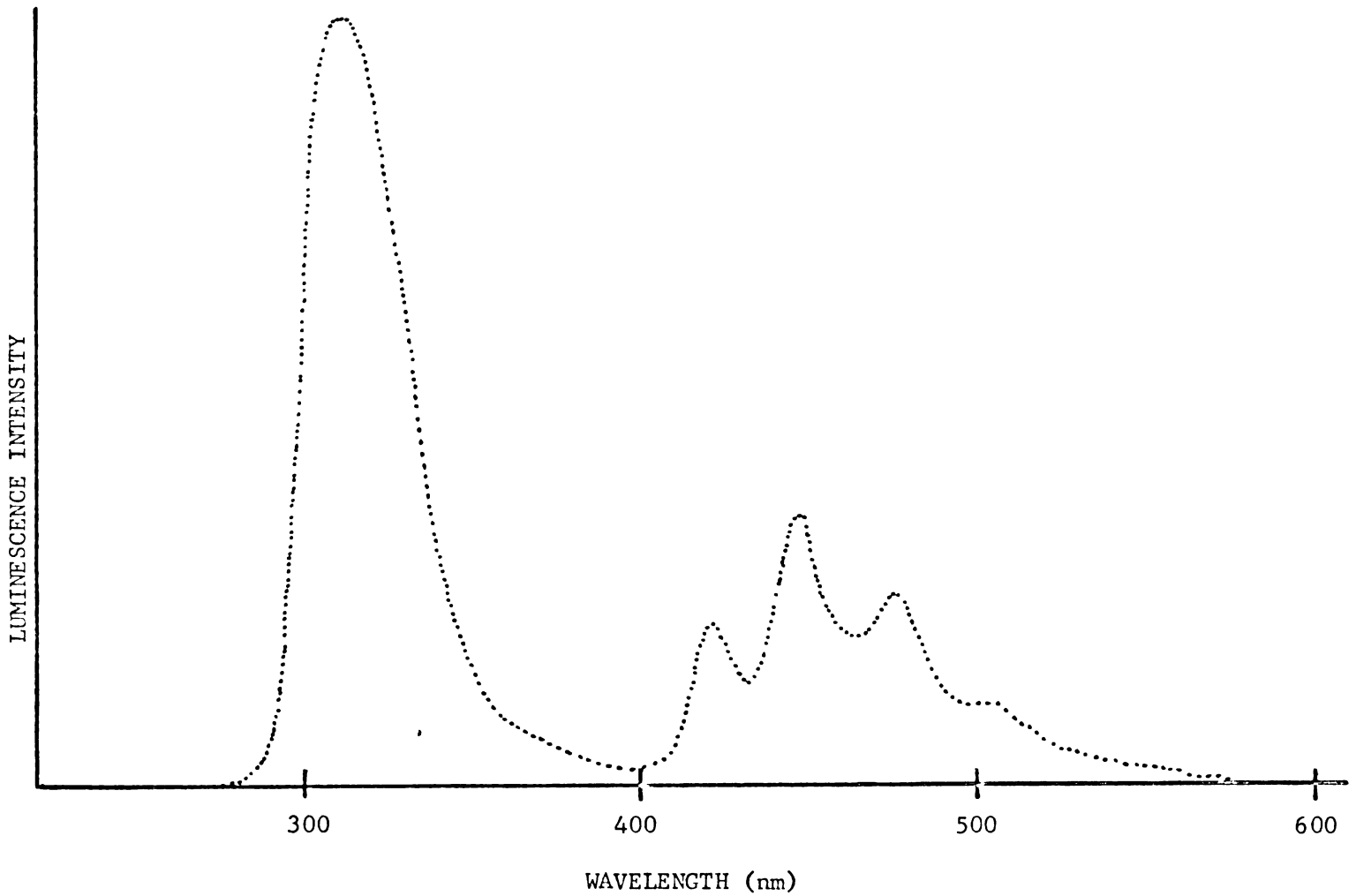

Figure 21. Emission Spectrum of 2-Azaindole in 3MP at 77°K.

room temperature. Both luminescence bands are fluorescence bands, the long wavelength fluorescence (F_2) is absent in both ether and water. The broad, structureless fluorescence F_2 band arises from a tautomer which is formed due to excited state double proton transfer that occurs in the 7-azaindole hydrogen bonded dimer (in 3MP) and the 7-azaindole-alcohol complex (in ethanol).

Excited State Dipole Moment Studies

The methods for the determination of excited state dipole moments can be combined into four groups: (1) The method of spectral shifts[13,14,19,23] based on the study of the displacements of the frequencies of electronic transitions and such shifts are obtained from the analysis of the absorption and luminescence spectra in different media. (2) The method of electrical polarization of fluorescence[24,25]. Here the degree of polarization of the emission by solutions of the test substances in a powerful electric field is measured, i.e., ultimately the anisotropy of the emission in the direction of the field orienting the molecules is investigated. (3) The method of electrical dichroism[26,27]. Here the dichroism of the absorption by molecules in a solution placed in a powerful electric field is studied, i.e., the anisotropy of absorption in the direction of the orienting field is considered. (4) The method based on the investigation of the splitting of the fine rotational structure of the absorption bands of certain molecules in the gas phase in a powerful electric field (the Stark effect, which includes not only the excited electronic states but also the ground state)[28].

The method I used here is the spectral shifts method. The method is based on the application of McRae[13] and Ooshika[23] formula to determine the difference between shifts of absorption and fluorescence bands under the

conditions such that the orientation relaxation time of the solvent molecules is much less than the lifetime of excited fluorescence state. The following simple expression is then obtained:

$$\Delta\bar{\nu}_{a-f} = 2(\mu_e - \mu_g)^2\{(D-1)/(D+2) - (n^2-1)/(n^2+2)\}/a^3hc \qquad (21)$$

as the first term of equation 11.

The solvent I used here for this study is a polar but non-hydrogen bonding solvent CH_2Cl_2, also assuming the cavity radius a in Onsager's[19] theory of the reaction field to be 3 Å for indole[29] and azaindoles. No hypotheses concerning the relative orientation of the moments μ_g and μ_e but only the $|\Delta\mu|$ are considered. The Stokes shifts and the calculated $|\Delta\mu|$ are given in Table 8. The $|\Delta\mu|$ for indole and most of the azaindoles are in the range of 5-6D, except 5-azaindole which showed a value of 9.1D and 2-azaindole showed a value of 4.5D. Aza-substitution along the long axis seems to perturb the system most.

Excited State pK Studies

As we already pointed out in the introduction, Weller has shown that electronic excitation may change drastically the acid-base properties of a molecule.

If equilibrium is established during the excited state lifetime, then the pK_a^* and pK_b^* can be determined in a way analogous to the spectrophotometric determination of the ground state pK's by fluorometric titration. For this reason we have studied the fluorescence intensity as a function of pH (corrections were made for changes in the absorption spectra) for indole and azaindoles. The results of indole and 7-azaindole are now discussed, the data for other azaindoles are summarized in Table 9.

Indole

As we see, at both low and high pH, indole fluorescence is quenched.

Table 8. Lowest Singlet Excited State Dipole Moments of Indole and Azaindoles.

Compound	Stoke Shift (cm^{-1})	$\Delta\mu$ (D)	μ_g (D)	μ_e (D)
Indole	3666	5.0	2.3*	7.3
2-Azaindole	3109	4.5	1.8*	6.3
3-Azaindole	4531	5.5	4.0*	9.5
4-Azaindole	3944	5.2		
5-Azaindole	12048	9.1		
7-Azaindole	5924	6.4	3.6**	10.0

* Reference 17

** Reference 10

In the high pH region the quenching is ascribed to the ionization of the pyrrolic hydrogen according to the reaction

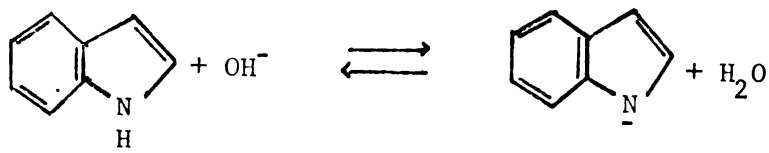

From the midpoint of the titration curve (Figure 22), one get a pK_b*=12.3. Exactly the same number was obtained by Donckt[30]. The excited state pK_b* = 12.3 should be compared to the ground state pK_b = 16.97[31], which shows that indeed the pyrrolic hydrogen acidity has considerably increased in the excited state.

In the low pH region the quenching is considered to be due to protonation of the pyrrolic nitrogen according to the reaction

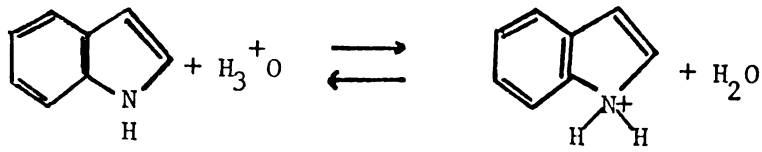

In the same way one gets a pK_a* = 1.8, in very good agreement with the value pK_a* = 1.7 by Bridges and Williams[32].

7-Azaindole

From the fluorometric titration of 7-azaindole (Figure 23), we get a pK_a* = 4.7. Besides the quenching upon increase of the concentration of H_3^+O and approximately below pH = 4, a new fluorescence band appears with a maximum around 450 nm which is ascribed to the cation resulting from the protonation of the N_7 position. Since the cation is emitting it provides us with an opportunity to test if euqilibrium is really established in the excited state if a pK_a* = 4.7 is really representing the true thermodynamic pK_a*.

Following the method of Weller as derived in the introduction that

Figure 22. Fluorimetric Titration Curve of Indole (25°C)

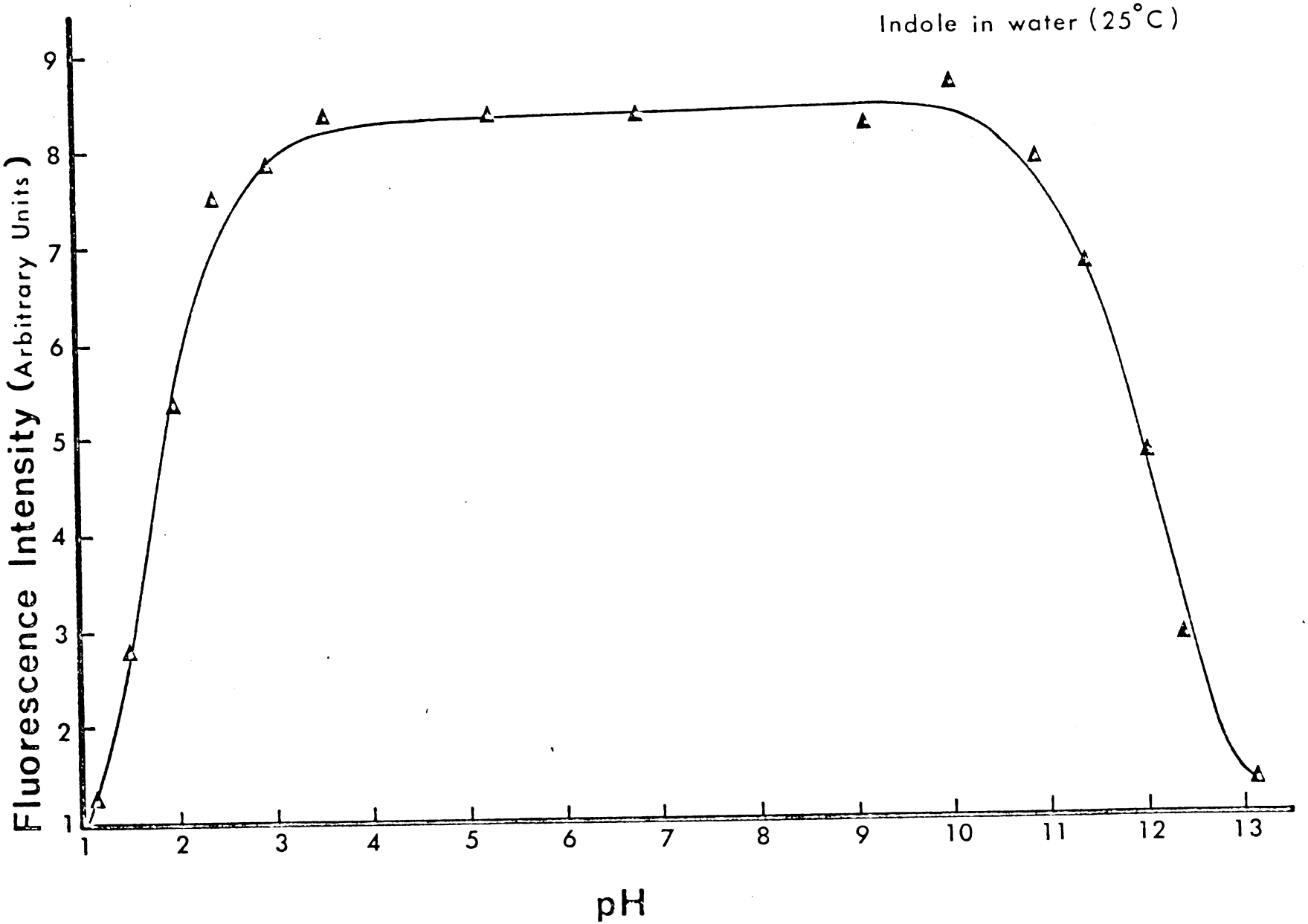
Indole in water (25°C)
Fluorescence Intensity (Arbitrary Units)
9
8
7
6
5
4
3
2
1
1
2
3
4
5
6
7
8
9
10
11
12
13
pH

Figure 23. Fluorimetric Titration Curve of 7-Azaindole.

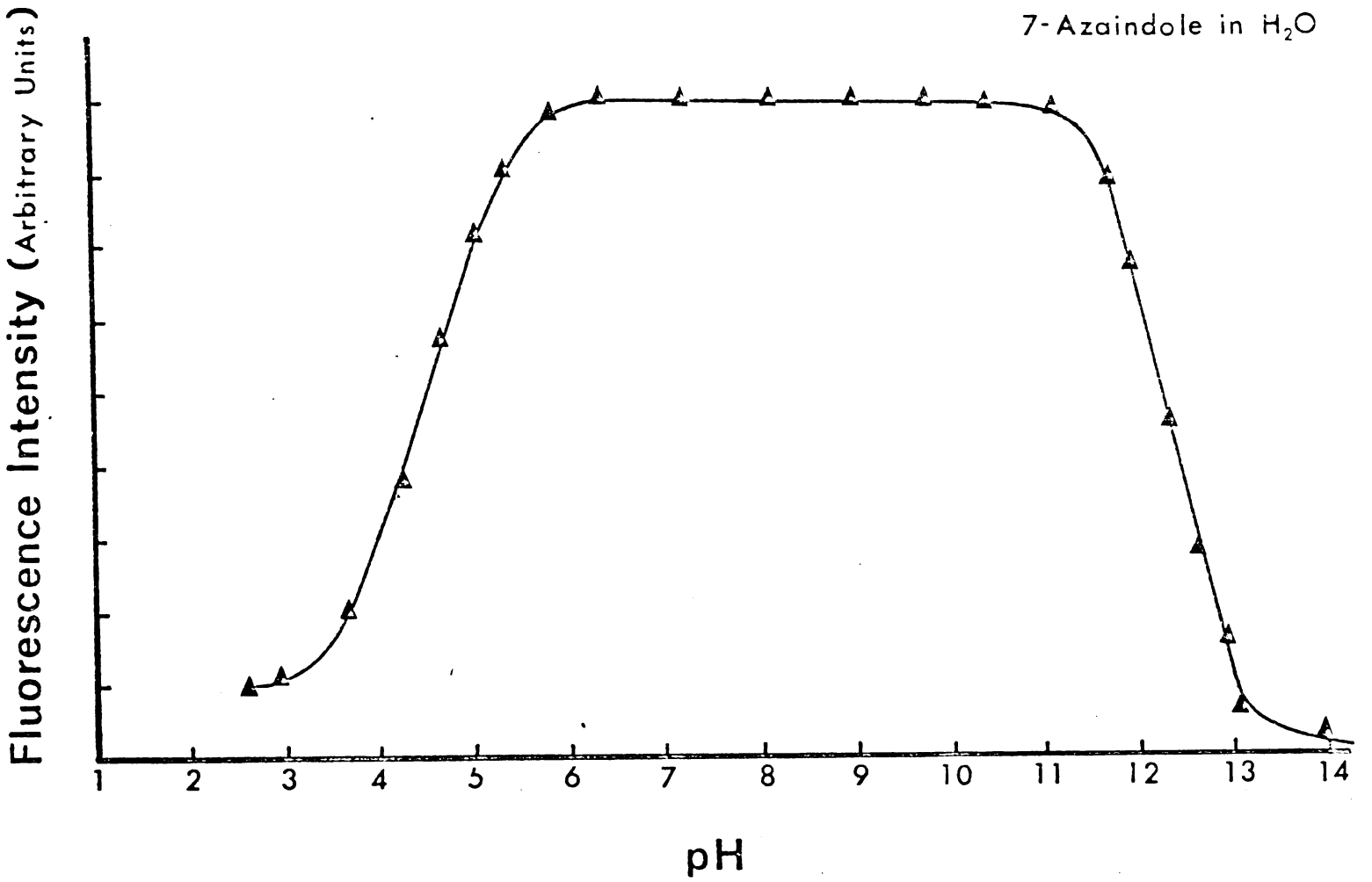
7-Azaindole in H_2O
Fluorescence Intensity (Arbitrary Units)
1
2
3
4
5
6
7
8
9
10
11
12
13
14
pH

$$\Delta pK = pK - pK^* = (\Delta E - \Delta E')/2.303RT \qquad (22)$$

Using our data we find (25°C) that $pK_a - pK_a^* = 3.1$. This result coupled with Albert and Adler's[33] ground state $pK_a = 4.59$ gives us a thermodynamic $pK_a^* = 7.7$. This shows that the rate of protonation is slow compared to the deactivation rate of the excited state and so in the excited state the ground state equilibrium is insignificantly perturbed.

The fluorimetric titration result for the pK_b^* is 12.3, the same as the one found for indole. Longworth et al.[34] gave a $\Delta pK_b = 7.5$ for indole. If we accept the ΔpK_b as being the same for 7-azaindole as for indole, which appears reasonable, then the thermodynamic $pK_b^* = 9.5$ to be compared with the titrametric $pK_b^* = 12.3$. This indicates that the ground state equilibrium is perturbed significantly ($pK_b = 17$) during the excited state lifetime but complete thermodynamic equilibrium is not attained.

A table showing the comparison of the titrametric pK's and thermodynamic pK's is give in Table 9. In general the fluorimetric titration need not give the true thermodynamic pK because it depends on the rate with which equilibrium is attained. If the acid-base reaction is slow then equilibrium may not be attained during the exicted state lifetime and in this case the titrametric pK will be closer to the ground state pK. For example compare the titrimetric and thermodynamic pK_a^* for 7-azaindole.

The pK_b^* for all compounds studied is lower than 16.97, the ground state pK_b of indole. If we make the assumption that all these compounds have approximately the same pK_b as indole that means that the indolic hydrogen becomes more acidic in the lowest excited state (^1L_b). This fact is in accord with charge density calculations using Pariser-Parr-Pople method where it is found that in the ^1L_b state there is a reduction

Table 9. Lowest Singlet Excited State pK's of Indole and Azaindoles.

Compound	pK_a	pK^*_a(titration)	pK^*_a(thermodynamic)
Indole	1	1.8	
2-Azaindole	1.22	2.4	5.6
3-Azaindole	5.33	5.5	8.5
4-Azaindole	6.94	4.5	
5-Azaindole	8.26		
7-Azaindole	4.59	4.7	7.7

Compound	pK_b	$\Delta\rho_1(^1L_b)$	pK^*_b(titration)	pK^*_b(thermodynamic)
Indole	16.97	-0.098	12.3	
2-Azaindole			11.9	11.6
3-Azaindole		-0.239	11.9	
4-Azaindole		-0.097	12.5	
5-Azaindole		-0.059	11.3	
7-Azaindole		-0.033	12.3	9.5**

** Reference 34

($\Delta\rho_1$) of charge density compared to ground state in position 1. Since Pariser-Parr-Pople method is π-electron method, no correlation can be made with the protonation reaction (pK_a) which involves the σ -electron system.

BIBLIOGRAPHY

BIBLIOGRAPHY

1. Pardee, A. B., Shore, V. G., and Prestidge, L. S. (1956) Biochim. Biophys. Acta 21, 406.

2. Sundaram and Sarma (1957) Current Sci. 26, 13.

3. Kidder, G. W., and Dewey, V. C. (1955) Biochim. Biophys. Acta 17, 288.

4. Potts, N. S. (1952) J. Chem. Phys. 20, 809.

5. Platt, J. R. (1949) J. Chem. Phys. 17, 484.

6. Klevens, H. B., and Platt, J. R. (1949) J. Chem. Phys. 17, 470.

7. Kasha, M. (1950) Disc. Farad. Soc. 9,14.

8. Hollas, J. M. (1963) Spectrochim. Acta 19, 753.

9. Gordon, R. D., and Yang, R. F. (1970) Can. J. Chem. 48, 1722.

10. Wagner, R. W. (1971) Ph. D. Thesis, Michigan State University.

11. Bayliss, N. S., and McRae, E. G. (1954) J. Phys. Chem. 58, 1002.

12. Bayliss, N. S. (1957) J. Chem. Phys. 18, 980.

13. McRae, E. G. (1957) J. Phys. Chem. 61, 562.

14. Lippert, E. (1957) Z. Elektrochem. 61, 962.

15. Brealey, G. J., and Kasha, M. (1955) J. Am. Chem. Soc. 77, 4462.

16. Pimentel, G. C. (1957) J. Am. Chem. Soc. 79, 3323.

17. McClellan, A. L. (1963) in "Table of Experimental Dipole Moments". W. H. Freeman and Company, San Francisco and London.

18. Bellamy, L. J. (1956) in "The Infra-Red Spectra of Complex Molecules". Methuen and Company.

19. Onsager, L. (1936) J. Am. Chem. Soc. 58, 1486.

20. Weller, A. (1961) in "Progress in Reaction Kinetics", Vol. 1, Chap. 7 Pergamon Press, London.

21. Weller, A. (1958) Z. Physik. Chem. 18, 163.

22. Weller, A. (1952) Z. Elektrochem. 56, 662.

23. Ooshika, Y. (1954) J. Phys. Soc. Japan 9, 594.

24. Czekalla, J., and Meyer, K. (1961) Z. Phys. Chem. (Frankfurt) 27, 185.

25. Liptay, W., (1963) Naturforsch 18a, 705.

26. Liptay, W., and Czekella, J. (1961) Z. Elektrochem. 65, 721.

27. Labhart, J. (1961) Helv. Chim. Acta 44, 447.

28. Lombardi, J., Campbell, D., and Klemperer, W. (1967) J. Chem. Phys. 46, 3482.

29. Mataga, N., Torihashi, Y., and Ezumi, K. (1964) Theoret. Chim. Acta (Berl.) 2, 158.

30. Donckt, E. V. (1969) Bull. Soc. Chim. Belges. 78, 69.

31. Yagil, G. (1962) J. Phys. Chem. 71, 1034.

32. Bridges, J. W., and Williams, R. T. (1968) Biochem. J. 107, 225.

33. Adler, T. K., and Albert, A. (1960) J. Chem. Soc. 1794.

34. Longworth, J., Rahn, R., and Shulman, R. (1966) J. Chem. Phys. 45, 2930.